

AN ABSTRACT OF THE THESIS OF

DOUGLAS GLENN HILL for the M.S. in Electrical Engineering.

Date thesis is presented March 4, 1965

Title MEDIUM FREQUENCY SOLID-STATE CORRELATOR

Abstract approved_

Redacted for privacy

Periodic signals hidden in noise may be detected by using correlation techniques. This thesis presents a study of how correlation is approximated statistically, and carried out electronically.

The ability to detect periodic signals in noise, using correlation, is justified mathematically in the first portion of the thesis. The discussion is based on the autocorrelation function and its characteristics. Considerable attention is given to showing the relationship between the time average of the autocorrelation function and its statistical average. This is necessary since statistical approximations are used in the actual correlator. It is possible to determine the frequency of the input signal, hidden in noise, by autocorrelation.

The circuit design used to approximate the autocorrelation function is discussed in detail in the next section of the thesis. The system design uses all solid state components, including several field effect transistors.

The last section of the thesis discusses the expected correlator output, compares this with the actual output, and explains any discrepancies between the two. Data is presented to verify a frequency response of 2kc - 30kc, and to show the quality of signal detection when the input N/S ratio is as high as 10db.

The detection of a periodic pulse train in noise, and the possible application of this technique to communication line fault location is also presented.

MEDIUM FREQUENCY
SOLID-STATE CORRELATOR

by

DOUGLAS GLENN HILL

A THESIS

submitted to

OREGON STATE UNIVERSITY

in partial fulfillment of
the requirements for the
degree of

MASTER OF SCIENCE

June 1965

APPROVED:

Redacted for privacy

Associate Professor of Electrical Engineering
in Charge of Major

Redacted for privacy

Head of Department of Electrical Engineering

Redacted for privacy

Dean of Graduate School

Date thesis is presented March 4, 1965

Typed by Lois Shrader

ACKNOWLEDGMENT

The author wishes to express his gratitude to Associate Professor Leonard J. Weber for his suggestions and guidance throughout the course of this thesis.

I would also like to thank Donald L. Amort for the components, equipment, and suggestions he supplied.

TABLE OF CONTENTS

| | |
|--|----|
| Introduction | 1 |
| Basic Concepts | 4 |
| What is Correlation | 4 |
| Periodic Functions | 4 |
| Random Functions | 7 |
| Relationship Between Ensemble Averages and Time Averages | 11 |
| Periodic Signal Detection in Random Noise | 17 |
| Electronic Approximation of Correlation | 19 |
| The System | 25 |
| Master Timer | 26 |
| Sampler-A | 27 |
| Zero Order Hold-A | 31 |
| Amplifier Inverter-1(AI-1) | 33 |
| T-step Delay Introduction | 34 |
| Voltage Step Generator | 34 |
| Miller Sweep Generator-1(MSG-1) | 37 |
| Schmitt Trigger-1 | 37 |
| Brief Review of T-step Delay | 41 |
| Other Comments | 46 |
| Pulse Width Modulation | 46 |
| Pulse Height Modulation | 48 |
| Integrator-Summer | 49 |
| Read-out | 51 |

| | |
|--|----|
| Integrator Reset Circuit | 51 |
| System Evaluation | 54 |
| Frequency Response | 54 |
| Noise Response | 62 |
| Periodic Pulse Train Detection in Noise | 66 |
| In Retrospect | 78 |
| Conclusion | 79 |
| Appendix | |
| Appendix I - Important Basic Circuits and Calculations | 82 |
| Appendix II - Correlator Test Operation Instructions | 86 |
| Appendix III - Circuit Specifications | 89 |
| Appendix IV - Complete Block Diagram of Medium Frequency Solid State Correlator | 91 |
| Appendix V - Complete Circuit Diagram of Medium Frequency Solid State Correlator | 93 |

LIST OF FIGURES

| <u>Figure</u> | | <u>Page</u> |
|---------------|---|-------------|
| 1 | Pictorial representation of autocorrelation for $\tau = \tau_1$. | 5 |
| 2 | Autocorrelation of sine wave. | 7 |
| 3 | Autocorrelation function of random process. | 10 |
| 4 | Ensemble aggregate of random function. | 12 |
| 5 | PDF for random functions. | 15 |
| 6 | Ensemble aggregate of random function. | 16 |
| 7 | Autocorrelation function of signal + noise. | 19 |
| 8 | Sampling of $f_1(t)$. | 20 |
| 9 | Simplified block diagram of correlator. | 22 |
| 10 | Characteristic waveforms of electronic correlator. | 23 |
| 11 | Master timer output. | 27 |
| 12 | Ideal sampler. | 28 |
| 13 | Sampler-A. | 28 |
| 14 | Sampling Pulse Generator-A output. | 29 |
| 15 | Sampler-A equivalent circuit when saturated. | 29 |
| 16 | Sample waveform of 0.4v signal pulse 0.7v noise. | 32 |
| 17 | Zero order hold. | 33 |
| 18 | Binary pulse counter output waveforms. | 35 |
| 19 | Voltage step generator. | 36 |

| | | |
|----|---|----|
| 20 | Step generator voltage. | 38 |
| 21 | Miller sweep-1 voltage. | 38 |
| 22 | Schmitt trigger-1. | 39 |
| 23 | τ -step delay waveforms. | 40 |
| 24 | Schmitt trigger-1 output voltage. | 42 |
| 25 | Schmitt trigger-1 output voltage amplified by T_{21} . | 43 |
| 26 | Comparison of sampling pulse train a and b. | 44 |
| 27 | Comparison of sampler A and B output waveforms. | 45 |
| 28 | Miller sweep-2 voltage. | 45 |
| 29 | Pulse width modulated pulse train. | 47 |
| 30 | Diode gate. | 48 |
| 31 | Pulse width and height modulated pulse train. | 50 |
| 32 | Integrator reset circuit. | 53 |
| 33 | Autocorrelation of periodic sinusoid, $f_1(t)$. | 54 |
| 34 | Possible frequency response of correlator with $\tau_k = 5\mu\text{sec}$. | 56 |
| 35 | Graph- Relationship between time taken for τ shift and actual value of τ on horizontal axis, vs. number of points produced on correlation curve for τ shift. | 58 |
| 36 | Autocorrelation of 2kc sinusoid. No noise. | 59 |
| 37 | Autocorrelation of 5kc sinusoid. No noise. | 59 |
| 38 | Autocorrelation of 10kc sinusoid. No noise. | 60 |
| 39 | Autocorrelation of 20kc sinusoid. No noise. | 60 |

| | | |
|----|---|----|
| 40 | Autocorrelation of 30kc sinusoid. No noise. | 61 |
| 41 | Distortion of sinusoid by addition of noise. | 63 |
| 42 | PDF for true random noise. | 64 |
| 43 | Autocorrelation of 10kc sinusoid. No noise. | 67 |
| 44 | Autocorrelation of 10kc sinusoid. + noise. N/S ratio 0db. | 67 |
| 45 | Autocorrelation of 10kc signal + noise. N/S ratio 2db. | 68 |
| 46 | Autocorrelation of 10kc signal + noise. N/S ratio 5db. | 68 |
| 47 | Autocorrelation of 10kc signal + noise. N/S ratio of 10db. | 69 |
| 48 | Autocorrelation of 10kc signal + noise. N/S = 10db. | 69 |
| 49 | Autocorrelation of noise. No signal. | 70 |
| 50 | Autocorrelation of 2kc signal + noise. N/S ratio = 10db. | 70 |
| 51 | Autocorrelation of 5kc signal + noise. N/S ratio = 10db. | 71 |
| 52 | Autocorrelation of 10kc signal + noise. N/S ratio = 10db. | 71 |
| 53 | Autocorrelation of 20kc signal + noise. N/S = 10db. | 72 |
| 54 | Autocorrelation of 30kc signal + noise. N/S = 10db. | 72 |
| 55 | Autocorrelation function for periodic pulse train. | 73 |
| 56 | Distortion of pulse train by addition of random noise. | 74 |

| | | |
|----|---|----|
| 57 | Autocorrelation of Figure 56(a) and (b). | 75 |
| 58 | Voltage waveform for pulsed communications line terminated with open circuit. | 76 |
| 59 | Frequency spectrum of periodic waveform of rectangular pulses. | 77 |
| 60 | FET and its equivalent circuit. | 83 |
| 61 | Miller sweep generator-1. | 84 |
| 62 | Miller sweep generator-1 reset. | 85 |
| 63 | Complete block diagram of medium frequency solid state correlator. | 90 |
| 64 | Complete circuit diagram of medium frequency solid state correlator. | 93 |

NOMENCLATURE

| | |
|------------------|---|
| AI-n | Amplifier Inverter-n ¹ |
| CON-n | Variable Resistor |
| Diff | Differentiator |
| FET _n | Field Effect Transistor |
| Int | Integrator |
| MSG-n | Miller Sweep Generator-n ¹ |
| MSGR-n | Miller Sweep Generator Reset-n ¹ |
| OA | Operational Amplifier |
| PDF | Probability Density Function |
| PG-n | Monostable Multivibrator-n ¹ |
| PW | Pulse Width |
| SPG-A | Sampling Pulse Generator-A |
| SPG-B | Sampling Pulse Generator-B |
| T _n | Transistor _n ¹ |
| TC | Time Constant |

¹ n is number of specific device

MEDIUM FREQUENCY SOLID-STATE CORRELATOR

INTRODUCTION

An information signal carried by a communications channel is often hidden in excessive amounts of noise. Noise is considered to be any unwanted signal other than the original information signal being transmitted. If the information content of the transmitted signal is to be recovered, the noise must be reduced or eliminated. The purpose of this thesis is to show, both mathematically and electronically, how correlation techniques are used to detect periodic signals in random noise.

The basic mathematical concepts associated with correlation are presented in the first section of the thesis. The discussion is based on the autocorrelation function and its characteristics. Autocorrelation is the correlation of a function of time with itself. The function of time to be correlated may be a periodic signal, random noise, or the combination of both. If the function to be correlated contains a periodic signal the autocorrelation function will be a periodic signal of the same frequency. A periodic signal hidden in random noise can therefore be detected and its frequency calculated directly from the autocorrelation function.

To correlate electronically, statistical approximations to the

autocorrelation function are used. Considerable emphasis is therefore placed on the relationship between time functions and their statistical approximations. This is followed by a basic outline of the electronic system used to perform autocorrelation.

The second section of the thesis explains in detail the circuitry used in the correlator. The entire design is solid state with field effect transistors (FET) used extensively to provide very high input impedance where needed. The FET are expensive but without them the system would have been much more difficult to design. Most of the conventional circuitry, such as multivibrators, sweep generators, and differentiators, are discussed only to the extent of where the circuit appears in the system and the function it performs.

The quality and limitations of the above system are considered in the final portion of the thesis. The expected results are discussed first and then compared to the experimental results. Frequency limitations of the system are explained and output waveforms from 2 kc - 30 kc are shown. Periodic signals in the above frequency band can be detected when the noise (N) level (rms volts) is over three times greater than the signal (S) level (rms volts) ($N=3.14S$, $N/S=10\text{db}$).

With further circuit sophistication the frequency response could be extended to 2 kc - 75 kc and periodic signals could probably

be detected with a N/S ratio equal to 20db. The added circuitry needed to provide the above improvements would not increase the cost of the system appreciably.

The appendix contains a complete description of circuits and calculations referred to in the body of the thesis. Correlator specifications, operating instructions, and complete block and circuit diagrams are also included.

BASIC CONCEPTS

The mathematical formulation and application of correlation to the electronic detection of periodic signals in random noise will be presented in this portion of the thesis.

What is Correlation

Correlation can be applied to three types of time functions; periodic, aperiodic, and random. This thesis will be concerned only with periodic and random functions; both of utmost importance to communications engineering.

Periodic Functions

For periodic time functions correlation is defined (4, p. 9) as

$$\frac{1}{T_1} \int_{-T_1/2}^{T_1/2} f_1(t) f_2(t+\tau) dt$$

where $f_1(t)$ and $f_2(t)$ have the same fundamental frequency, and τ is a continuous time displacement in the range $(-\infty, \infty)$, independent of t .

For the special case when $f_1(t) = f_2(t)$ autocorrelation is defined as

$$(1) \quad \phi_{11}(\tau) = \frac{1}{T_1} \int_{-T_1/2}^{T_1/2} f_1(t) f_1(t+\tau) dt$$

As shown by Equation (1), and Figure 1 below, autocorrelation consists of three basic operations:

- a) Shifting $f_1(t)$ with respect to itself over values of τ from $(-\infty, \infty)$.
- b) The continuous multiplication of $f_1(t)f_1(t+\tau)$.
- c) Finding the average value of (b) over some time interval T .

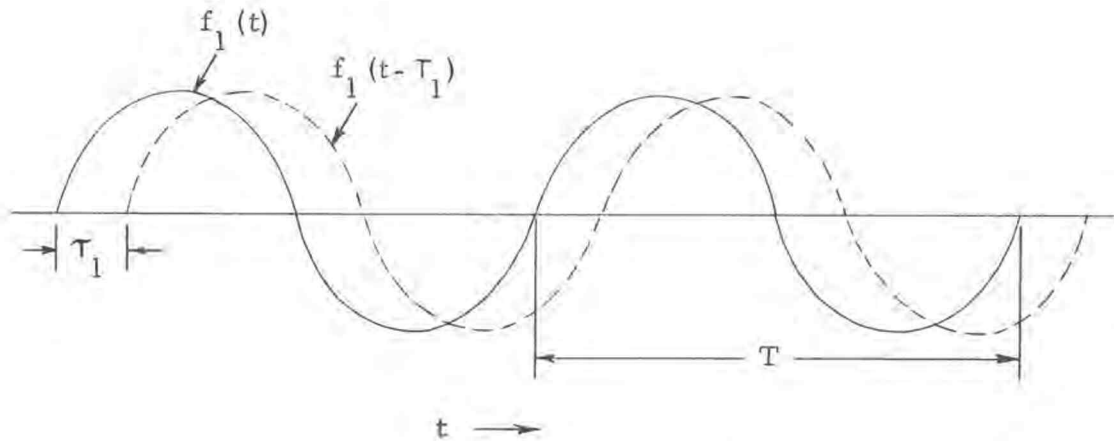


Figure 1. Pictorial representation of autocorrelation for $\tau = \tau_1$.

Positive values of τ result in shift to the left, whereas negative values of τ shift $f_1(t)$ to the right.

A summary of the properties of the autocorrelation function for periodic signals are listed below.

- a) It is an even function $\phi_{11}(\tau) = \phi_{11}(-\tau)$.
- b) The frequency of the function $f_1(t)$, to be correlated, need not be known.
- c) The autocorrelation function is assumed to exist for every value of the argument.
- d) The autocorrelation function retains all harmonics of the given function, $f_1(t)$, but discards all their phase angles.
- e) The frequency of $\phi_{11}(\tau)$ is the same as $f_1(t)$.

The above discussion can be summarized further by including an example that will illustrate the above principles.

Autocorrelation of a Sinusoid

$$f_1(t) = A \cos(\omega_1 t + \theta)$$

The autocorrelation function is

$$\phi_{11}(\tau) = \frac{1}{T_1} \int_{-T_1/2}^{T_1/2} A \cos(\omega_1 t + \theta) A \cos(\omega_1 t + \theta + \tau) dt$$

$$\phi_{11}(\tau) = \frac{A^2}{2} \cos \tau$$

The graphs of $f_1(t)$ and $\phi_{11}(\tau)$ are given below in Figure 2.

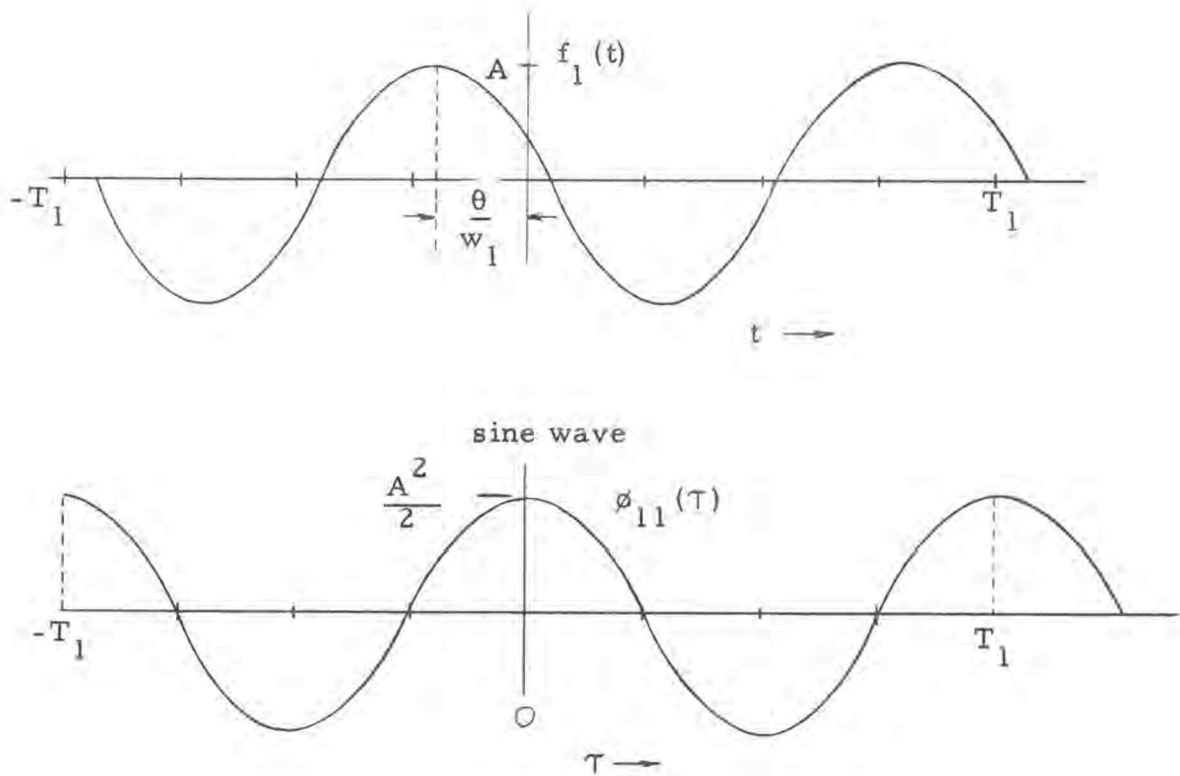


Figure 2. Autocorrelation of sine wave.

Random Functions

Periodic signals are simple to evaluate since a mathematical equation can be written to describe their characteristics. There is no mathematical equation, however, that can be written to describe a random function. To analyze a random function assume it has

been going on from the infinite past to the present. Next assume the random function is being produced by many independent sources. The output from each source provides a portion of the entire function. The entire function will be referred to as the ensemble, and the output from each source an ensemble member (4, p. 50). From this aggregate of member ensembles it is possible to find the probability density function (PDF) for a random function. If the function is stationary¹ the PDF will be the same for the infinite future as it was for the infinite past. It thus becomes possible to predict, with a certain probability, the future value of the random function. From the above assumptions and definitions it will be proven, later on in the discussion, that the statistical average for a random function is equal to the time average of each ensemble member. At that time the importance of the terms ensemble, ensemble member, and stationary will become more evident.

If $f_1(t)$ is a member function of the ensemble, its autocorrelation function is

$$\phi_{11}(\tau) = \lim_{T \rightarrow \infty} \frac{1}{T} \int_{-T/2}^{T/2} f_1(t) f_1(t+\tau) dt$$

¹When the complete set of probability densities are independent of the origin from which time is measured.

Autocorrelation of a random function follows the same three basic steps as for periodic functions; shifting, multiplication, and averaging.

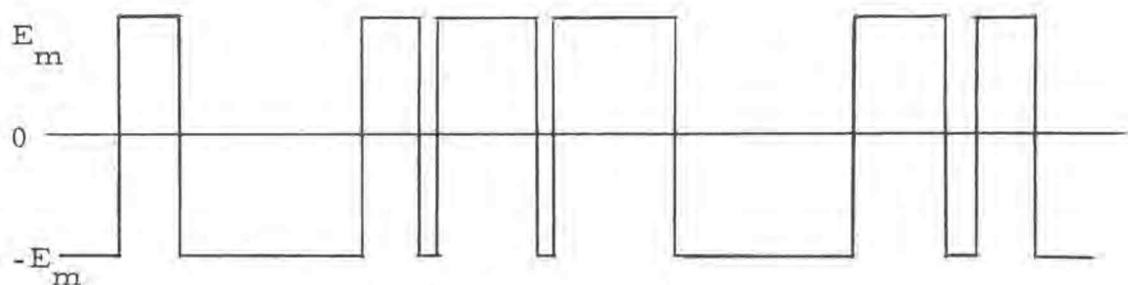
A summary of properties for the autocorrelation function of a random process is shown below.

- a) It is an even function $\phi_{11}(\tau) = \phi_{11}(-\tau)$.
- b) Its value at the origin ($\tau=0$) is the mean square value of the random function

$$= \lim_{T \rightarrow \infty} \frac{1}{T} \int_{-T/2}^{T/2} f_1(t)^2 dt$$

- c) It tends to zero as the argument tends to infinity if the random function contains no d.c. or periodic components $\phi_{11}(\infty) = 0$.
- d) Its value at the origin is the one and only maximum value in magnitude i. e. $\phi_{11}(0) > |\phi_{11}(\tau)|$ for $\tau \neq 0$.
- e) The autocorrelation function is assumed to exist at every value of the argument.
- f) It is continuous everywhere if it is continuous at the origin.

To help solidify the above discussion the following example is given.

Autocorrelation of Random Function


Random Wave with two possible values.

The Poisson probability distribution (4, p. 53) describes the above waveform. The autocorrelation function is

$$\phi_{11}(\tau) = E_m^2 e^{-2k|\tau|}$$

where k = average number of random zero crossings per second.

The autocorrelation function for $k = 1000$ and $E_m = 1$ volt is shown below in Figure 3.

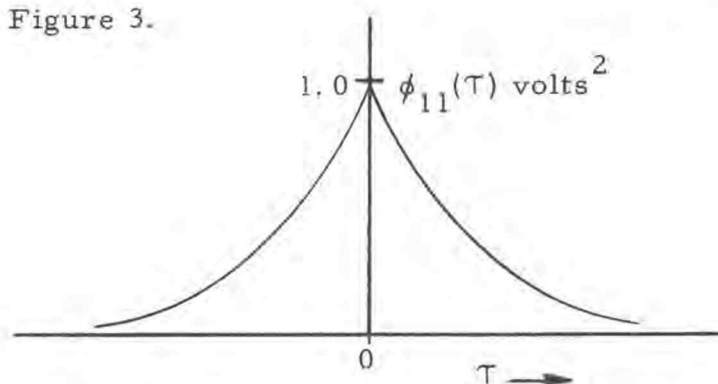


Figure 3. Autocorrelation function of random process.

Relationship Between Ensemble Averages and Time Averages

As discussed earlier for periodic (p. 4) and random (p. 7) functions the final step in finding the autocorrelation function is averaging. In statistical theory of communications there are two kinds of averages; time averages and ensemble (statistical) averages. The ensemble average of a random function can be predicted if its PDF is known. Without the PDF the time average can be estimated only from past behavior because its future cannot be predicted precisely (4, p. 122). The following discussion considers in detail the equality of a time average and ensemble average, and the subsequent relationship to autocorrelation.

Assume a stationary random process $f(t)$. Divide the infinite past of $f(t)$ into M equal parts of duration T , as shown in Figure 4.

As discussed earlier (p. 8) each waveform $(1, 2, 3, \dots, M)$ is assumed to be generated by an independent source, and is an ensemble member of the original function of time.

The time average of each ensemble member is

$$(2) \quad \lim_{T \rightarrow \infty} \frac{1}{T} \int_{-T}^0 f(t) dt$$

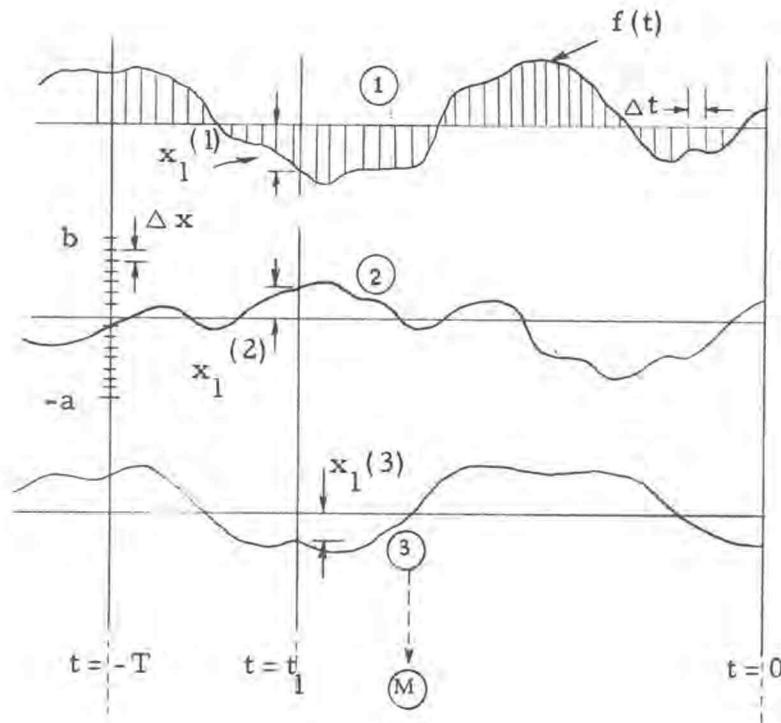


Figure 4. Ensemble aggregate of random function.

Since each ensemble member is an independent random function, the time average will be the same for each member. To establish the relation between the average value of an ensemble member as a function of time t , and the average value of amplitude of the ensemble at time $t = t_1$, refer back to Figure 4. Divide the interval $(-T, 0)$ into $n = T/\Delta t$ parts. The time average of an ensemble member from $(-T, 0)$ is

$$(3) \quad \overline{f(t)}^1 = \lim_{\substack{T \rightarrow \infty \\ \Delta t \rightarrow 0}} \frac{f(-\Delta t) + f(-2\Delta t) + \dots + f(-i\Delta t) + \dots + f(-n\Delta t)}{T/\Delta t}$$

$$\overline{f(t)} = \lim_{\substack{T \rightarrow \infty \\ \Delta t \rightarrow 0}} \left[\frac{f(-\Delta t) + f(-2\Delta t) + \dots + f(-i\Delta t) + \dots + f(-n\Delta t)}{T} \right] \Delta t$$

which is

$$\overline{f(t)} = \lim_{T \rightarrow \infty} \frac{1}{T} \int_{-T}^0 f(t) dt$$

The values of $x_1^{(1)}, x_1^{(2)}, \dots, x_1^{(i)}$ for the amplitude of each ensemble member of $t = t_1$ must equal the values of $f(-\Delta t), f(-2\Delta t), \dots, f(-i\Delta t)$, even though not in the same order. Assuming the amplitude of $f(t)$ varies from $-a$ to b this interval will be divided into elements of length Δx .

Given a large number, M , of ensemble members, each with amplitude $x_1^{(1)}, \dots, x_1^{(i)}, \dots, x_1^{(M)}$ there are

N_1 values falling in $(0, \Delta x)$

N_2 values falling in $(\Delta x, 2\Delta x)$

\vdots

in the positive range and

¹ $\overline{f(t)}$ indicates time average over an infinite interval.

N_{-1} values falling in $(0, -\Delta x)$

N_{-2} values falling in $(-\Delta x, -2\Delta x)$

\vdots

in the negative range. The statistical average (st. av.)

$$\text{st. av.} = \Delta x \frac{N_1}{M} + 2\Delta x \frac{N_2}{M} + \dots - \Delta x \frac{N_{-1}}{M} - 2\Delta x \frac{N_{-2}}{M} - \dots$$

is a close approximation to the average given in Equation 3. Dividing the ratios $(\frac{N_i}{M})$ by Δx and multiplying by Δx gives

$$(4) \quad \text{st. av.} = (\Delta x \frac{N_1}{M} \frac{1}{\Delta x} + 2\Delta x \frac{N_2}{M} \frac{1}{\Delta x} + \dots - \Delta x \frac{N_{-1}}{M} \frac{1}{\Delta x} - 2\Delta x \frac{N_{-2}}{M} \frac{1}{\Delta x}) \Delta x$$

The probability density function for Equation 4 is shown in Figure 5. The area of each element is given by $\frac{N_i}{M}$ so the height is $\frac{N_i}{M} \frac{1}{\Delta x}$. The curve is a legitimate PDF since the area under the curve is equal to 1.0, i.e., $\frac{N_1}{M} + \frac{N_2}{M} + \dots + \frac{N_i}{M} = 1$.

The average value of x for Equation 4 becomes

$$E(X) = \sum_i i \Delta x \left(\frac{N_i}{M} \frac{1}{\Delta x} \right) \Delta x$$

where $\frac{N_i}{M} \frac{1}{\Delta x} = \text{probability that the random function is equal to } i \Delta x$.

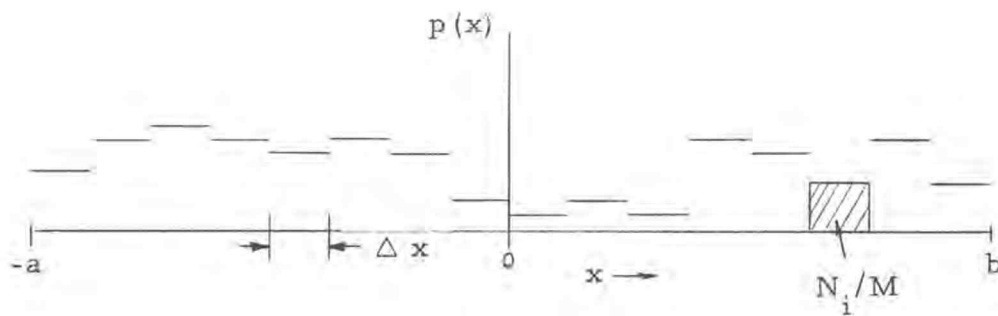


Figure 5, PDF for random functions.

If $M \rightarrow \infty$ and $\Delta x \rightarrow 0$ the continuous PDF for a random function is obtained and the average value over all x is given by

$$E(X) = \int_{-a}^b x P\{x\} dx$$

$$\lim_{\Delta x \rightarrow 0} \frac{N_i}{M} \frac{1}{\Delta x} \rightarrow P\{x\}$$

$$\Delta x \rightarrow dx$$

In a more general form

$$E(X) = \int_{-\infty}^{\infty} x P\{x\} dx$$

Thus it has been shown that in the limit

$$\lim_{T \rightarrow \infty} \frac{1}{T} \int_{-T}^0 f(t) dt = \int_{-\infty}^{\infty} x P\{x\} dx$$

It must also be assumed that the time average over the infinite future is equal to its value for the infinite past. Therefore

$$\lim_{T \rightarrow \infty} \frac{1}{2T} \int_{-T}^T f(t) dt = \int_{-\infty}^{\infty} x P\{x\} dx$$

It can be shown in a similar manner that the statistical average for autocorrelation is equal to the time average. To establish the relationship between the ensemble average for autocorrelation and the time average, again divide the random function into M ensemble members. Each ensemble member is then divided into an aggregate of values, each of duration Δt , as shown in Figure 6.

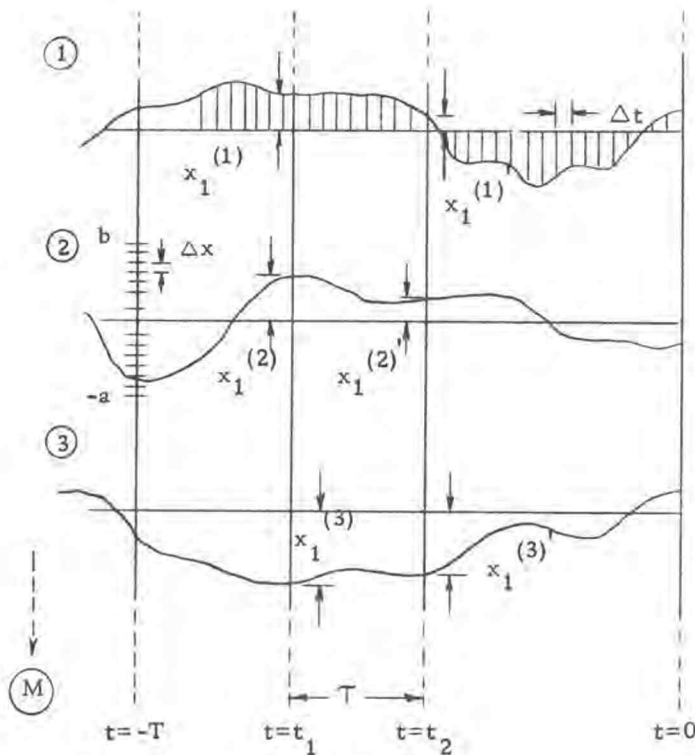


Figure 6. Ensemble aggregate of random function.

A time average of each ensemble member is determined by averaging the product of $f_1(t)$ at $t = 0, -\Delta t, -2\Delta t, \dots$ and $t = -T, -T-\Delta t, -T-2\Delta t, \dots$ respectively.

There are pairs of values $x_1^{(i)}, x_1^{(i)'} at $t = t_1$ and $t = t_2$ respectively, that correspond to the above pairs of time averages. A joint probability density function is formed by determining the number of pairs of values $(x_1^{(i)}, x_1^{(i)'})$ that fall between $(\Delta x, 2\Delta x), (2\Delta x, 3\Delta x),$ etc. In the limit as $M \rightarrow \infty$ and $\Delta x \rightarrow 0$ the joint probability function average is equal to the time average as $\Delta t \rightarrow 0$ and $T \rightarrow \infty$.$

$$(5) \quad \lim_{T \rightarrow \infty} \frac{1}{T} \int_{-T}^0 f(t)f(t+T)dt = \int_{-\infty}^{\infty} \int_{-\infty}^{\infty} x_1 x_2 p(x_1, x_2; T) dx_1 dx_2$$

Periodic Signal Detection in Random Noise

Communication channels are often hampered by noise. Noise is considered to be any unwanted signal other than the information being transmitted. Steps can be taken to minimize noise, but it can seldom be completely removed from the channel. The noise may become excessive at times and completely mask the information signal. The detection of such a signal in noise is a common communications problem.

The information signal must be periodic and the noise random

if correlation is to be used for detection. Let $f(t)$ be the sum of noise + signal

$$S(t) = \text{Signal}$$

$$f(t) = S(t) + N(t)$$

$$N(t) = \text{Noise}$$

The autocorrelation function of $f(t)$ is

$$\phi_{11}(\tau) = \overline{[S(t) + N(t)][S(t+\tau) + N(t+\tau)]}$$

$$\phi_{11}(\tau) = \overline{S(t)S(t+\tau) + S(t)N(t+\tau) + N(t)S(t+\tau) + N(t)N(t+\tau)}$$

$$= \phi_{SS}(\tau) + \phi_{SN}(\tau) + \phi_{NS}(\tau) + \phi_{NN}(\tau)$$

Consider first the two crosscorrelation¹ functions ($\phi_{SN}(\tau)$ and $\phi_{NS}(\tau)$). Set the time average equal to the ensemble average

$$\phi_{SN}(\tau) = \overline{S(t)N(t+\tau)} = \overline{\phi \delta}$$

where ϕ is the noise value and δ the value of signal. If the two time functions are independent then $\overline{\phi \delta} = \overline{\phi} \overline{\delta}$, where $\overline{\phi} = \overline{S(t)}$ and $\overline{\delta} = \overline{N(t+\tau)}$. Assuming $S(t)$ and/or $N(t)$ have zero means then

$$\phi_{SN} = \phi_{NS} = 0$$

¹ $f_1(t) \neq f_2(t)$

This reduces $\phi_{11}(\tau)$ to

$$\phi_{11}(\tau) = \phi_{SS}(\tau) + \phi_{NN}(\tau)$$

As already mentioned the value of $\phi_{NN}(\tau)$ will tend to zero after τ becomes large, leaving $\phi_{SS}(\tau)$. This will be a periodic function of exactly the same frequency as $S(t)$. The theoretical curve for autocorrelation function of a periodic sinusoid plus noise is shown in Figure 7.

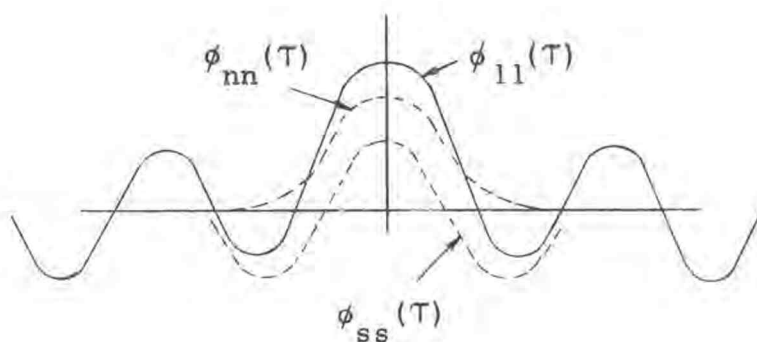


Figure 7. Autocorrelation function of signal + noise.

Electronic Approximation of Correlation

Now that the basic theory of autocorrelation has been discussed from a mathematical standpoint, it is possible to show how correlation can be approximated electronically.

Autocorrelation of a function $f(t)$ will be done electronically

by taking pairs of samples as shown in Figure 8 (4, p.262).

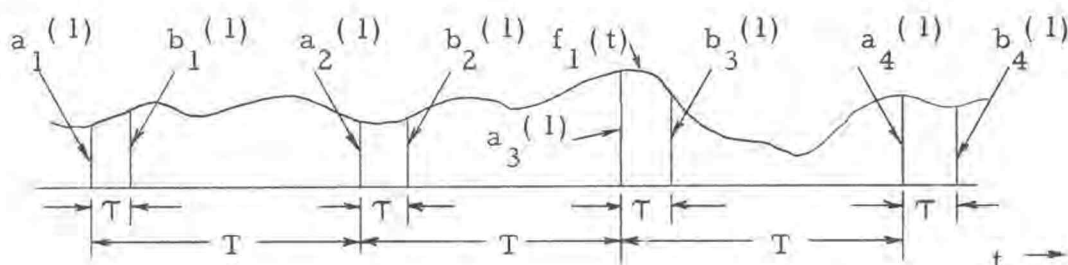


Figure 8. Sampling of $f_1(t)$.

Each interval T represents an ensemble member of $f(t)$ and N sample pairs $(a_n^{(1)}, b_n^{(1)})$ are taken separated by τ . If N is sufficiently large, the autocorrelation function is approximated by

$$(6) \quad \phi_{11}(\tau) \cong \frac{1}{N} \sum_{n=1}^N a_n^{(1)} b_n^{(1)}$$

As N approaches infinity Equation 6 becomes exactly equal to the autocorrelation function. Therefore

$$\begin{aligned} \phi_{11}(\tau) &= \lim_{T \rightarrow \infty} \frac{1}{T} \int_{-T}^0 f(t) f(t+\tau) dt = \int_{-\infty}^{\infty} \int_{-\infty}^{\infty} x_1 x_2 p(x_1, x_2; \tau) dx_1, dx_2 \\ &= \lim_{N \rightarrow \infty} \frac{1}{N} \sum_{n=1}^N a_n^{(1)} b_n^{(1)} \end{aligned}$$

An electronic correlator must provide sampling, T shift, multiplication, summation of N pairs of samples, and averaging. A simplified block diagram of such a correlator is shown in Figure 9. This block diagram in conjunction with the waveforms in Figure 10 will be used to explain the correlation procedure.

The MASTER TIMER provides a pulse train of set frequency which drives SAMPLING PULSE GENERATOR-A and a BINARY PULSE COUNTER. The BINARY PULSE COUNTER provides one output pulse for every N timer pulses. The T -STEP DELAY network is activated by the counter output and T is then increased T_k seconds. The sampling pulse train produced by SAMPLING PULSE GENERATOR-B is delayed an amount T from sampling pulse train-a. These two waveforms are shown in Figure 10(b). The function $f_1(t) = f_2(t)$ is sampled by SAMPLER A and SAMPLER B. The resulting waveforms are shown in Figure 10(c) and (d) respectively.

By use of PULSE HEIGHT MODULATION and PULSE WIDTH MODULATION it is possible to produce a pulse train whose amplitude is equal to $a_1^{(i)}$ and pulse width is proportional to $b_1^{(i)}$. The final waveform is shown in Figure 10(f).

The area under each pulse is equal to $a_i b_i$. An integrator is provided to integrate each pulse and sum the value of $a_1 b_1 + a_2 b_2 + \dots + a_N b_N$. After N pairs of samples have been taken

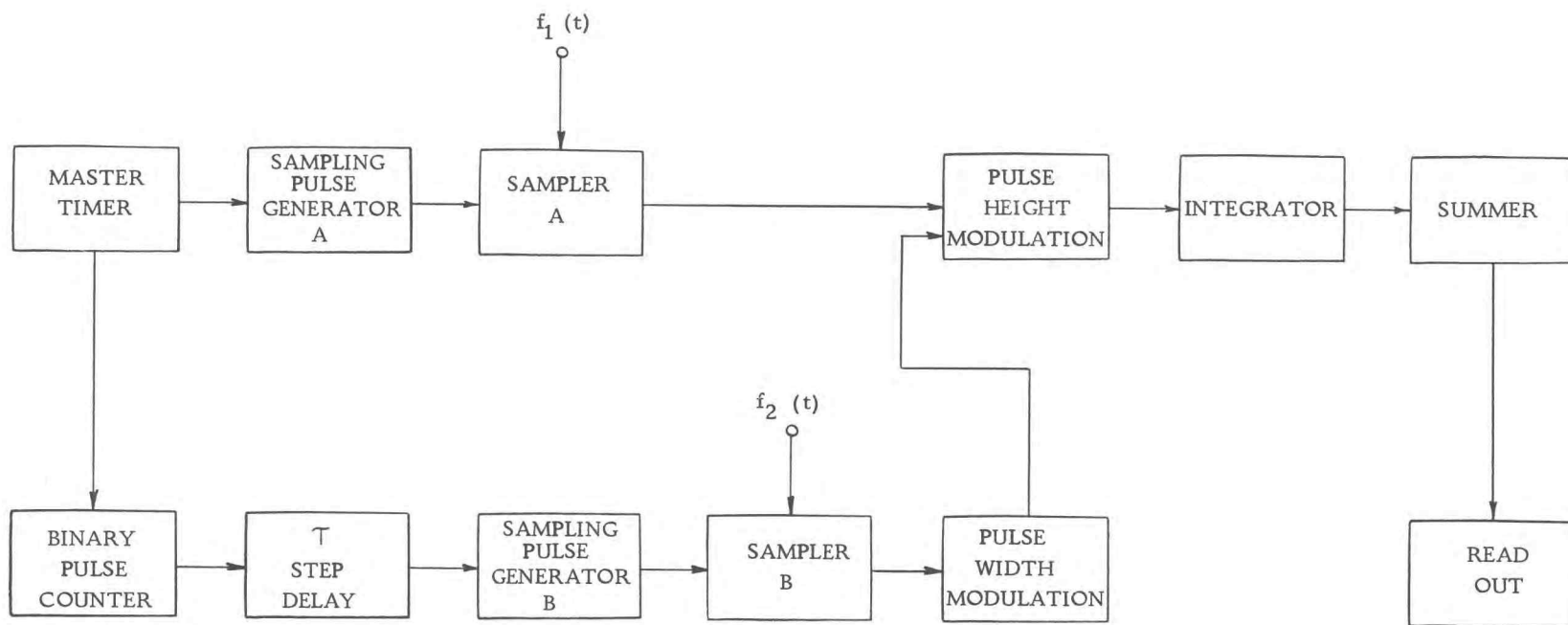


Figure 9. Simplified block diagram of correlator.

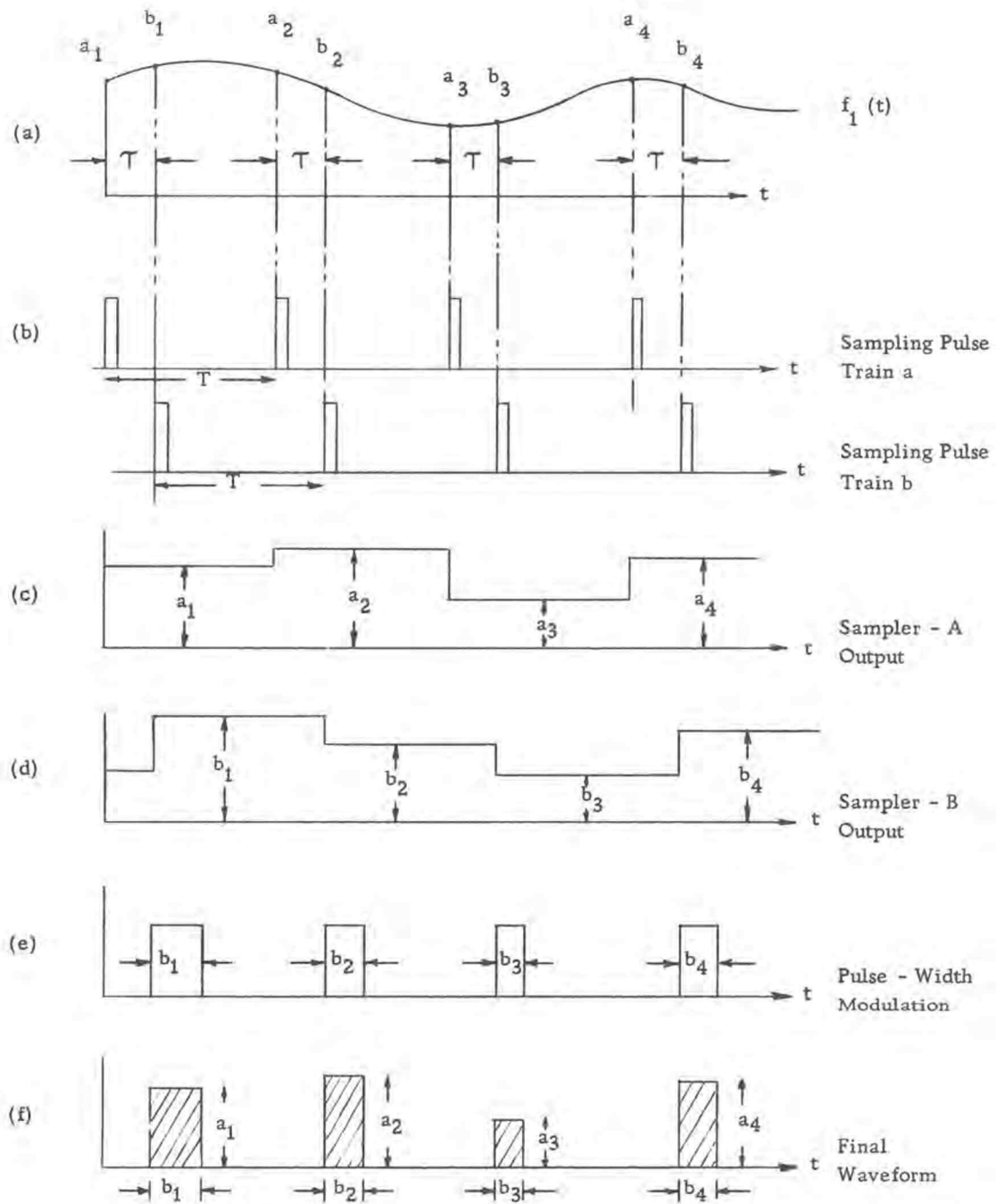


Figure 10. Characteristic waveforms of electronic correlator.

the integrator is reset to zero, τ is increased T_k seconds, and the process is repeated. The integrator output voltage after N pairs of samples have been summed provides one point of the cor-

relation curve. The averaging of $\sum_{i=1}^N a_i b_i$ is not carried out so the

output is proportional to $\phi_{11}(\tau)$.

THE SYSTEM

The mathematical theory of correlation and a basic outline of how correlation can be approximated electronically have been presented in the preceding section. Note that there are five basic operations to be performed by the correlator:

1. A timing circuit to regulate the rate sample pairs $(a_1, b_1), (a_2, b_2), \dots, (a_i, b_i), \dots, (a_N, b_N)$ are taken.
2. Sample $f_1(t)$ and obtain $a_1, a_2, \dots, a_i, \dots, a_N$.
3. Sample $f_1(t+\tau)$ and obtain $b_1, b_2, \dots, b_i, \dots, b_N$.
4. Produce a pulse train whose pulse width is proportional to b_i and height is equal to a_i .
5. Integrate the above pulses and sum the result over all i .

$$\text{i. e. } \sum_{i=1}^N a_i b_i$$

The circuitry needed to perform the above five operations will be of primary interest in the discussion that follows. The function each conventional circuit (monostable multivibrators, d.c. amplifiers, etc.) performs and where it appears in the system will be presented in the text of the thesis, but detailed explanations are

left to the references if the reader is interested in their operation. The system block diagram in Appendix IV p.90 and circuit diagram in Appendix V p.92 are used as a basis for the discussion.

Master Timer

The master timer consists of an astable multivibrator (8, p. 269) (T_1 & T_2), a one stage amplifier (T_3) biased in the active region, and a simple R-C differentiator. The output voltage from the multivibrator is amplified by T_3 to provide waveshaping and squaring. The amplifier output is then differentiated to provide a pulse train of positive and negative voltage spikes. The sequence of operations stated above are shown in Figure 11.

The time between positive pulses, T , is dictated by the amount of total shift T required to autocorrelate a particular input frequency. The lower frequency limit of the correlator is set at 2kc. The period of a 2kc periodic signal is 0.5 msec. A total shift in T of this amount will produce one cycle at the correlator output. (Refer to Figure 2, p.7) Thus T has been set at 1.3 msec.

The positive voltage spikes in Figure 11(c) are used to trigger MILLER SWEEP GENERATOR-1 (MSG-1) and SAMPLING PULSE GENERATOR-A (SPG-A). MSG-1 is part of the T -step delay circuit which will be discussed later. SPG-A is a conventional monostable pulse generator (8, p. 289) which produces sample pulse

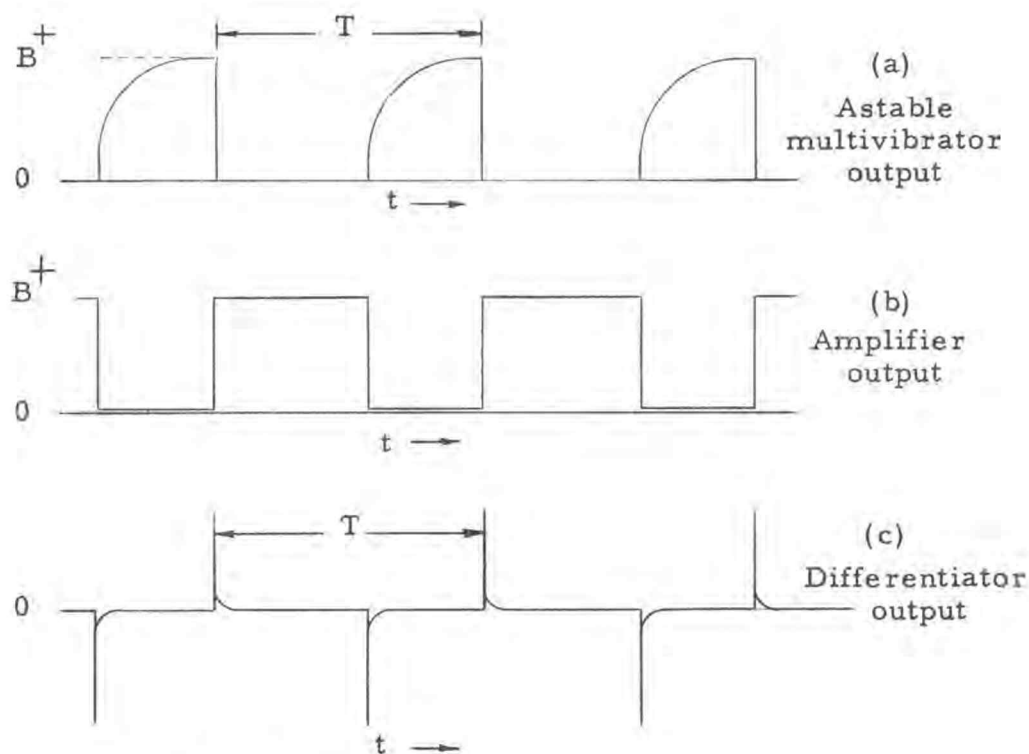


Figure 11. Master timer output.

train A. This pulse train consists of $1\mu\text{sec}$ wide positive pulses with period equal to T . The purpose of SPG-A is to trigger SAMPLER-A and a BINARY PULSE COUNTER.

Sampler - A

An ideal sampler is shown in Figure 12.

When S is closed C_s will charge to the value of $f_1(t)$ instantaneously. When S is open C_s will hold this charge indefinitely. When S is closed again C_s will charge to the new value of $f_1(t)$.

SAMPLER-A was designed to approximate ideal conditions and is shown in Figure 13. T_7 is used for switch S and is normally

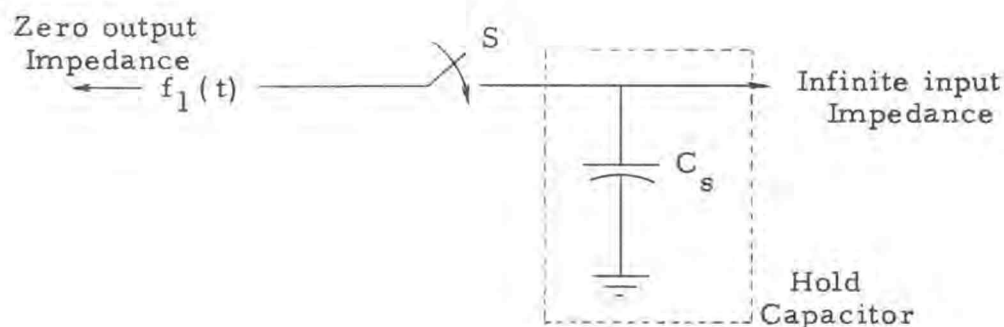


Figure 12. Ideal sampler.

"open", or in the cut-off region of operation. The bias voltage for T_7 is $f_1(t) + E_s$. The d.c. level is provided to keep the bias voltage positive since $f_1(t)$ has both negative and positive values. The output from SPG-A, as shown in Figure 14, forward biases the base-emitter junction of T_7 .

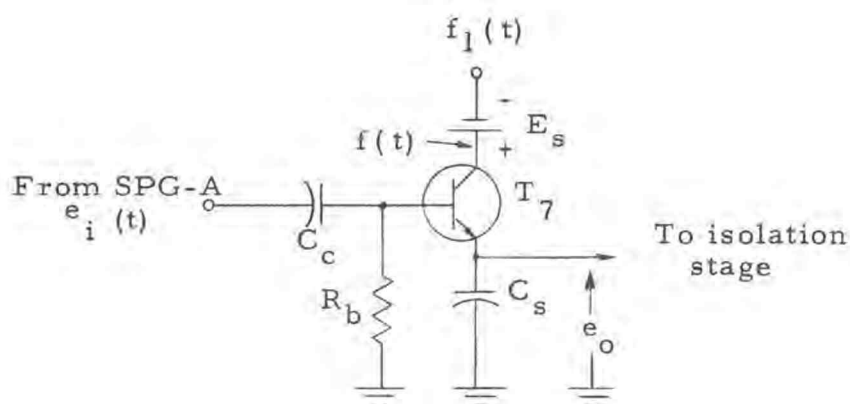


Figure 13. Sampler - A.

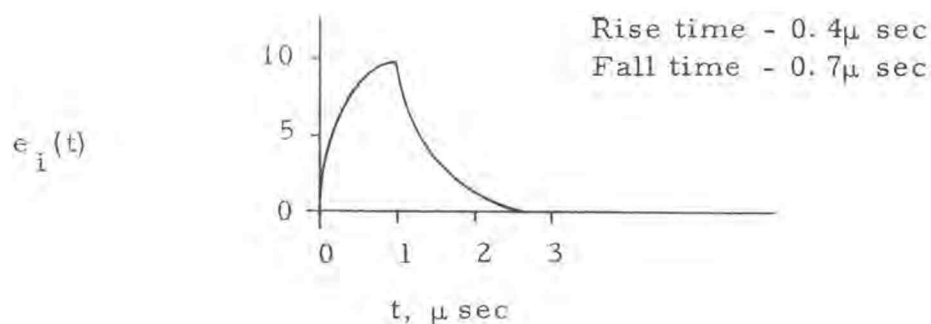


Figure 14. Sampling pulse generator - A output.

The capacitor, C_s , voltage follows $e_i(t)$ until the base voltage becomes greater than $f(t)$ ¹. When this condition occurs, the base-collector junction becomes forward biased and T_7 saturates. The equivalent circuit for Figure 13 during saturation is shown in Figure 15.

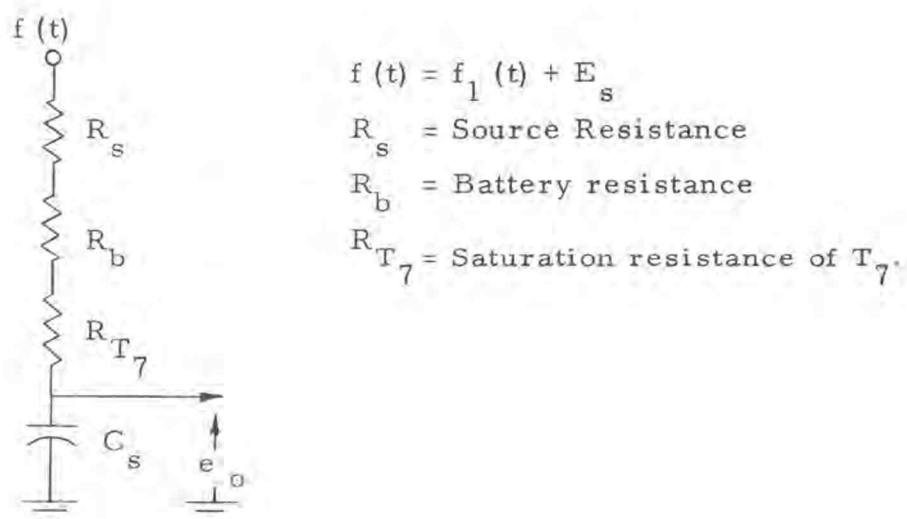


Figure 15. Sampler - A equivalent circuit when saturated.

¹ $f(t) = f_1(t) + E_s$

The value of $R_s + R_b$ is $\approx 1k\Omega$, depending on the type, and number, of signal generators used. The saturation impedance for a silicon transistor is several hundred ohms (4, p. 16). C_s will charge toward $f(t)$ with a time constant $(R_{T_7} + R_s + R_b) C_s$. The pk to pk value of $f_1(t)$ is limited to $2E_s$ volts. Anything greater than this would drive the collector negative and cause error in the sampler output. Assume E_s equals 3.5 volts and $f(t)_{\max} = 7.0$ volts. Referring back to Figure 14 it can be seen that $e_i(t) > f(t)_{\max}$ for approximately $1\mu\text{sec}$. The time required for C_s to reach $f(t)$ is $t = 4(T.C.)^1$. This criteria limits the value of C_s to

$$C_s \leq \frac{1\mu\text{sec}}{4(R_{T_7} + R_s + R_b)} \leq 160 \text{ picofarads}$$

A value of 50 pf is used to be sure C_s reaches $f(t)$ in $1\mu\text{sec}$.

As $e_i(t)$ falls below $f(t)$, T_7 returns to the active region and C_s charges very little. When $e_i(t)$ finally becomes less than 0.6v T_7 will cut-off. The voltage remaining on C_s is the value of $f(t)$. The voltage on C_s will follow $e_i(t)$ from zero to $e_i(\max)$ and back down to the voltage C_s has charged to. Due to this follower effect the input pulse, $e_i(t)$, will appear at the sampler output, but will not charge the capacitor. The resulting output waveform

¹T.C. = Time Constant

from SAMPLER-A is shown in Figure 16. Each time the sampler is triggered a new value of a_i is obtained.

When T_7 is OFF several things can happen to the charge on C_s . It can discharge through C_s itself, or through the input of the next stage to ground. Also, I_{co} (1, p. 14) will add more charge to C_s if it is of sufficient magnitude. If this leakage current is to cause no more than five per cent change in the capacitor voltage during the 1.3 msec T_7 is OFF, then the leakage current must be ≤ 13 nanoamps (see Appendix I, p. 82). For high quality silicon transistors the leakage current is normally less than this value.

To prevent discharge into the next stage a high input impedance circuit is used, which will now be discussed.

Zero-Order Hold-A¹

A field effect transistor follower configuration as shown in Figure 17, satisfies the requirement of high input impedance across C_s . The load impedance for FET₁ is the emitter follower circuit, T_8 . The time constant seen by C_s depends on the input impedance of the FET. For the Siliconix 2N2606 the input impedance is 2000 meg Ω .

¹ The term zero-order hold normally refers to the sampler and high input impedance stage across C_s . For this discussion only the high input impedance network is covered.

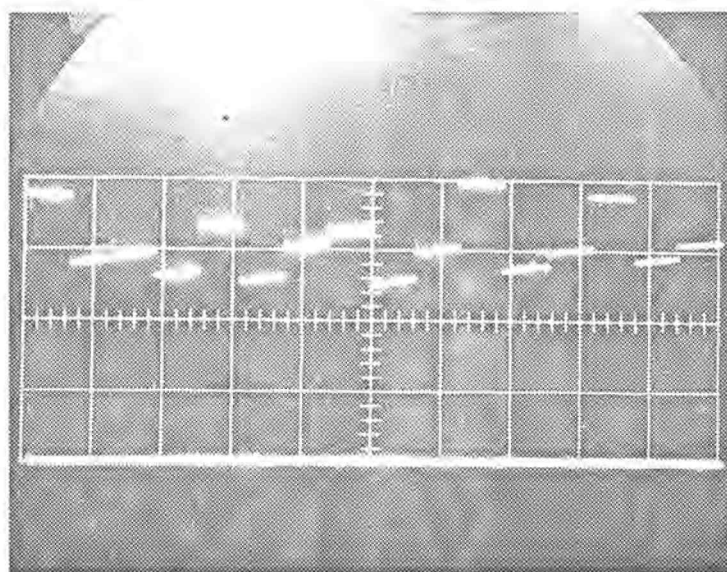


Figure 16. Sample waveform of 0.4 v signal plus 0.7v noise.

Abscissa - 2 msec/cm¹

Ordinate - 1 volt/cm

¹ One centimeter refers to one large division.

$$T.C. = (2000 \times 10^6) (50 \times 10^{-12})$$

$$T.C. = 100 \text{ msec}$$

Since C_s must hold charge for only 1.3 msec little discharge will occur.

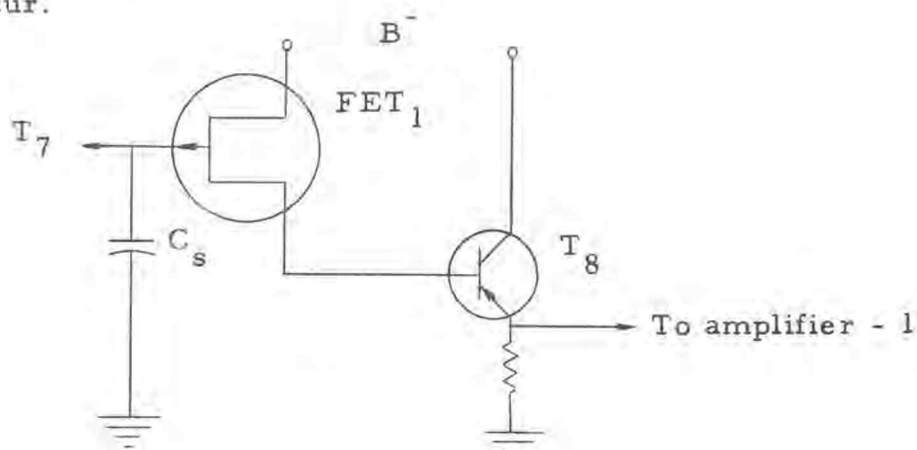


Figure 17. Zero order hold.

The zero order hold circuit does an excellent job of providing isolation between the sampler and amplifier inverter-1, which is a low input impedance (10k) device.

Amplifier Inverter-1 (AI-1)

To provide greater fluctuation in the correlator output voltage the sample waveform is amplified by T_9 . This also inverts the sampler voltage and consequently $\phi_{11}(\tau)$ will be inverted.

The previous discussion has shown how the values of $a_1, a_2, \dots, a_i, \dots, a_N$ are obtained. To provide sample pairs (a_i, b_i)

the time, t_2 , samples $b_1, b_2, \dots, b_i \dots b_N$ are obtained must be delayed T seconds from the time, t_1 , samples $a_1, a_2, \dots, a_i \dots a_N$ are taken. The circuitry used to generate this delay is now discussed.

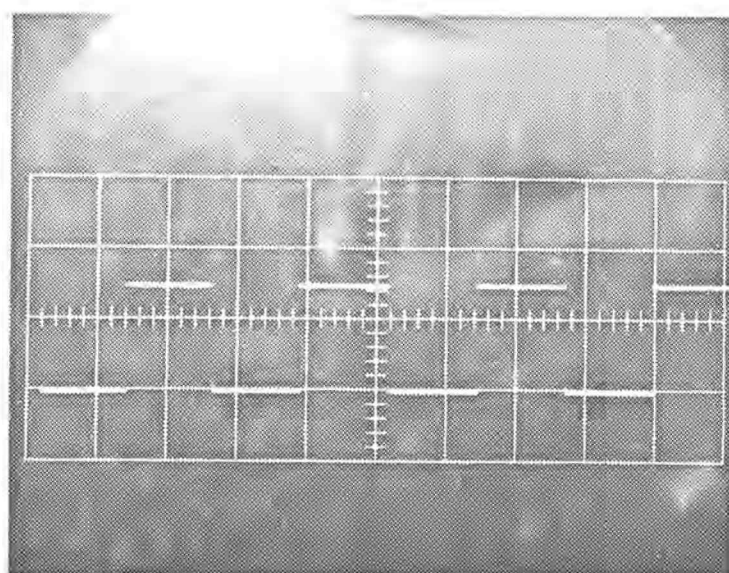
T-step Delay Introduction

A voltage step generator and Miller sweep generator provide the bias and trigger voltage, respectively, for a Schmitt trigger. The resulting output waveform produces the T -step delay. A detailed explanation of the process follows.

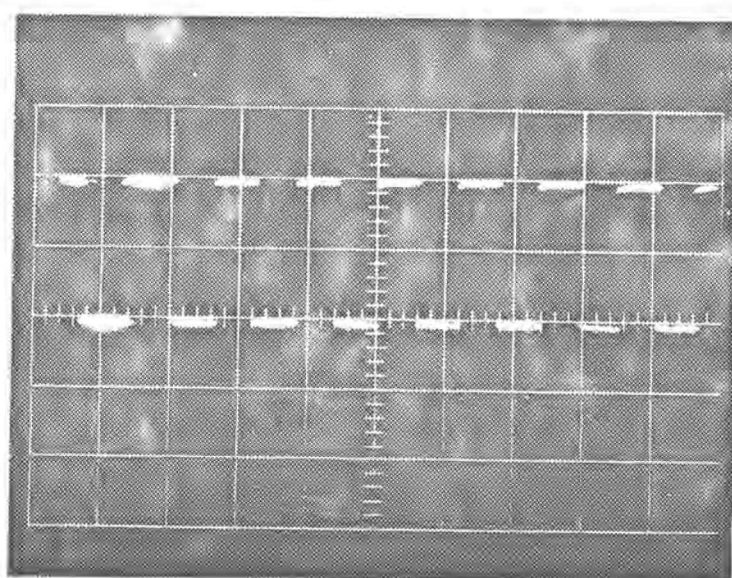
Voltage Step Generator

SPG-A triggers a BINARY PULSE COUNTER. The counter is conventional (8, p. 257) with 12 identical stages and diode steering. The first stage switches with every positive input pulse (every T seconds), and the last stage after every 2048 input pulses. The output from the first and last stage is shown in Figure 18. Waveform (b) is differentiated and the negative voltage spikes trigger MONO-STABLE PULSE GENERATOR-1(PG-1). The time between negative voltage spikes is

$$\begin{aligned} T_c &= (2^{12}) (T) \\ &= (4096) (1.3 \text{ msec}) \\ &= 5.33 \text{ seconds} \end{aligned}$$



(a)



(b)

Figure 18. Binary pulse counter output waveforms.

- Waveform (a) - Output from 1st stage
 Abscissa - 1 msec/cm
 Ordinate - 5 v/cm
- Waveform (b) - Output from 12th stage
 Abscissa - 5 sec/cm
 Ordinate - 5 v/cm

PG-1 drives the voltage step generator shown in Figure 19. Each pulse from PG-1 adds additional charge to C_G . A total of 220 pulses decreases the capacitor voltage from 0 to -S.V. max¹ exponentially. The charging path is a simple R-C network consisting of the forward resistance of D_1 and C_G .

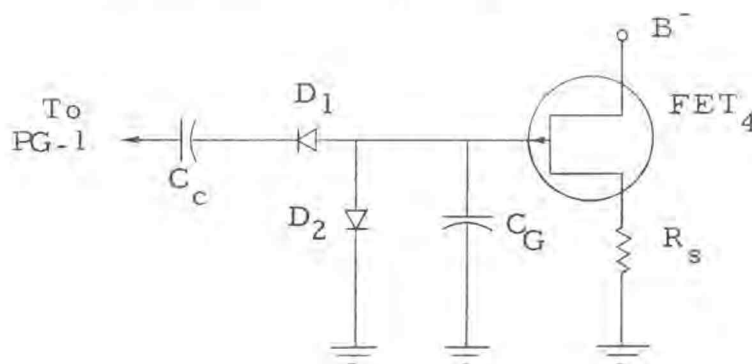


Figure 19. Voltage step generator.

The discharge time constant seen by C_G must be much greater than the time the capacitor is to hold charge (5.33 sec). The discharge time constant is equal to the parallel combination of the reverse resistance of D_2 (2000 meg Ω) and the input resistance of FET₄ (2000 meg Ω), multiplied by C_G .

$$\begin{aligned} T.C. &= (1000 \text{ meg}\Omega) (0.25\mu\text{fd}) \\ &= 250 \text{ sec} \end{aligned}$$

¹ Step generator voltage

No appreciable discharge will occur in 5.33 seconds.

The step generator voltage is shown in Figure 20. This step voltage provides the bias for Schmitt trigger-1.

Miller Sweep Generator - 1 (MSG-1)

The Miller sweep (8, p.178) is used to provide a linear voltage from 0 to -6 volts over a 1.3 msec time duration. The sweep voltage is reset to 0 volts by a MILLER SWEEP GENERATOR RESET circuit (see Appendix I, p.82) at the same instant SPG-A is triggered. The sweep voltage is shown in Figure 21. This voltage is clamped at zero volts and then applied to the base of T_{19} in Schmitt trigger-1.

Schmitt Trigger-1 (Figure 22)

This circuit is conventional and its principle of operation can be found in most basic electronics texts (9, p. 381). Its function is of enough importance to the system, however, to merit a detailed discussion.

It should be noted that the step generator voltage is inverted before it is applied to the Schmitt trigger. The step generator voltage decreases from 0 to -6 volts, whereas the Schmitt trigger bias increases from -6 to 0 volts.

Assume for the present the bias voltage is $-V.B.$ It will remain at this value for 5.33 seconds and then increase to

$-V.B. + \Delta(S.V.)^1$. During this period of time the sweep voltage in Figure 21 will repeat itself 4096 times. T_{20} is saturated when the

¹ $\Delta S.V.$ = change in step generator voltage.

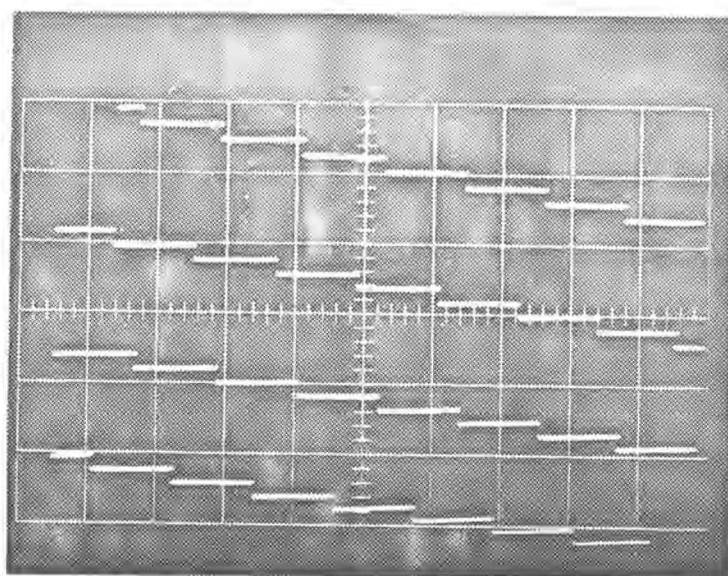


Figure 20. Step generator voltage. Above waveform is continuous, reading from left to right as sentences would normally be read in a book.

Abscissa - 5 sec/cm

Ordinate - 0.2 v/cm

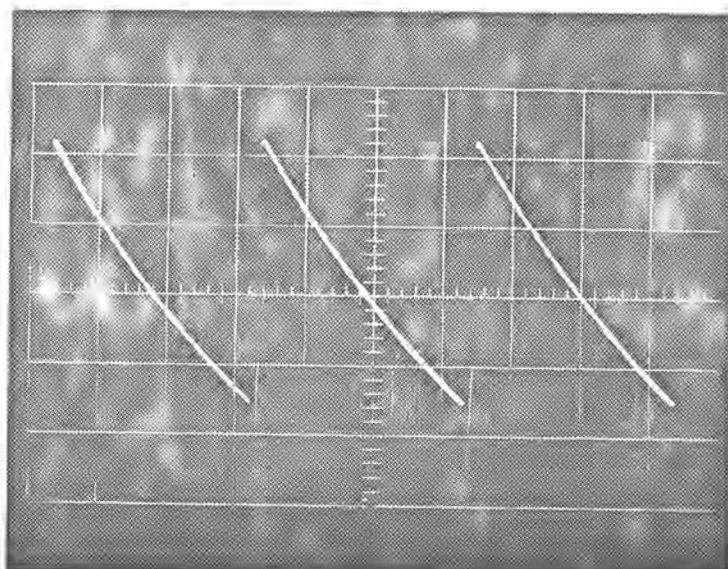


Figure 21. Miller sweep - 1 voltage.

Abscissa - 0.5 msec/cm

Ordinate - 2 v/cm

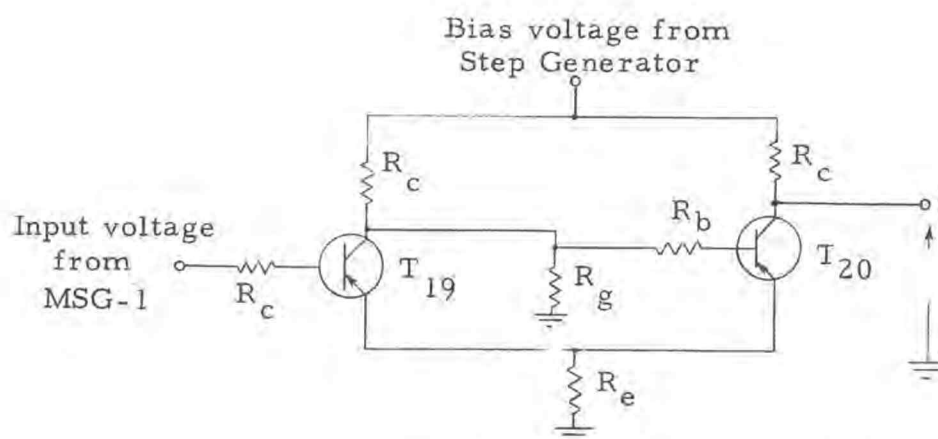
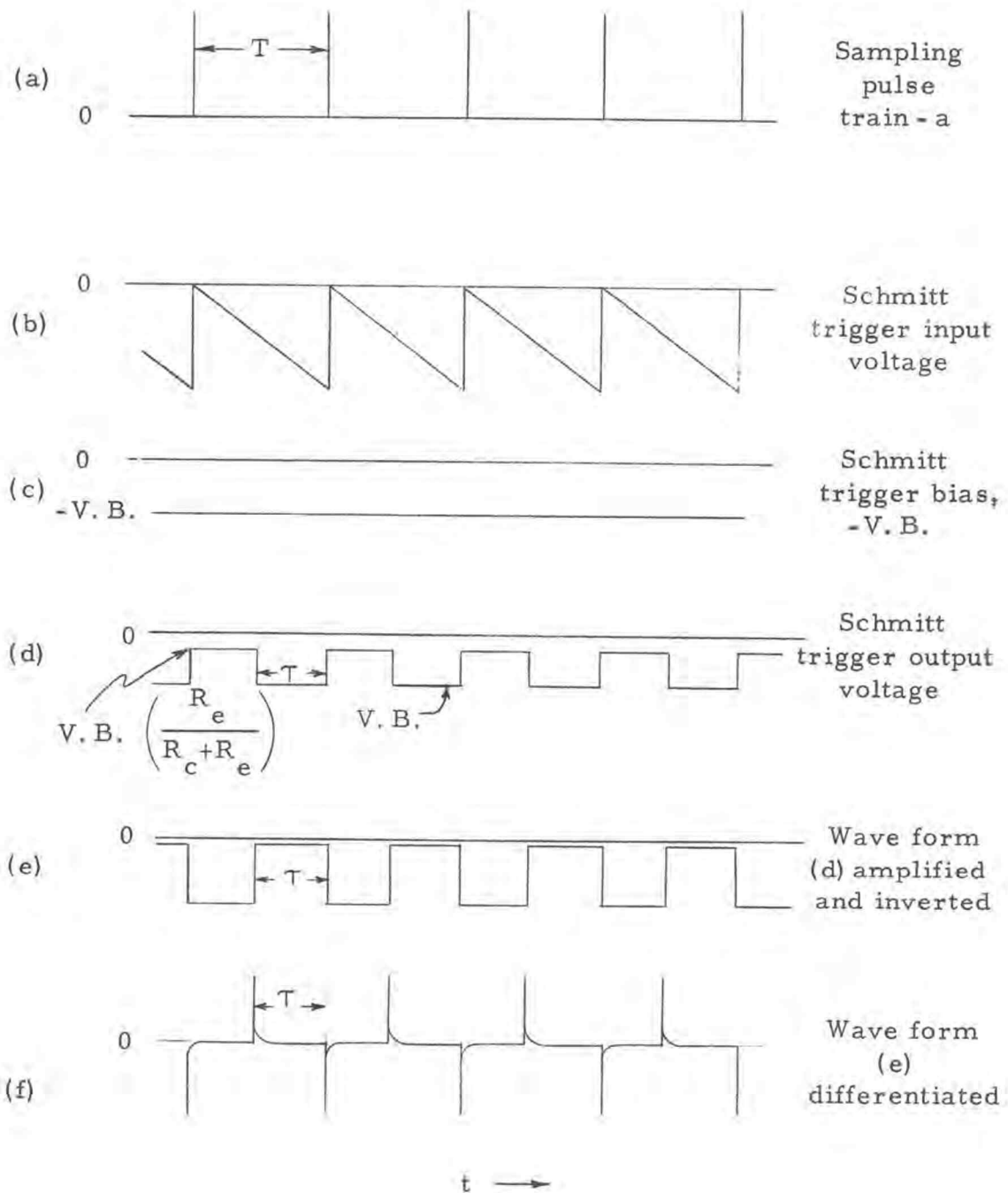


Figure 22. Schmitt trigger - 1.

sweep voltage is equal to zero. The emitter-ground voltage will be approximately $V_e = (-V.B) \frac{R_e}{R_e + R_c}$. T_{19} is in a cut-off condition and will remain cut-off until the sweep voltage becomes more negative than V_e . T_{19} starts to conduct the collector voltage of T_{19} will increase, and couple through R_e , R_g , and R_b to turn T_{20} OFF. T_{20} will remain OFF until the sweep voltage returns to zero. The voltage at the collector of T_{20} is equal to $-V_e + V_{ces}^1$ until it switches OFF. At this time the collector voltage will drop to $-V.B$, and remain at this value until the sweep voltage returns to almost zero and T_{20} again saturates. This process will repeat itself 4096 times for each discrete value of $-V.B$, and produce 4096 pulses of width τ as shown in Figure 23(d).

Figure 23 shows the sequence of operations described above. The schmitt trigger output (d) is amplified (e) and then

¹ V_{ces} = collector-emitter voltage during saturation.

Figure 23. τ -step delay waveforms.

differentiated (f). Notice how each positive spike in (f) is delayed $-\tau$ sec from sample pulse train-A. Picture the pulse train in (f) shifting to the left in discrete steps as V.B. is made less negative in discrete steps. When $-(V.B.) \frac{R_e}{R_e + R_c}$ is equal to the peak value of the sweep voltage the positive voltage spikes are in phase with sample pulse train-A. When $-(V.B.) \frac{R_e}{R_e + R_c}$ is equal to $(\text{sweep voltage})_{\max} / 4$ a shift of $-\tau = 3/4T$ is obtained. The amount of shift is controlled by $-V.B.$

The actual waveforms corresponding to Figure 23(d) and (e) are shown in Figure 24 and 25 respectively for various values of τ .

The differentiated waveform in Figure 23(f) triggers SAMPLING PULSE GENERATOR B (SPG-B). The shift, τ , between sample pulse train-A and B is shown in Figure 26.

SPG-A and SAMPLER-B are identical to SPG-A and SAMPLER-A respectively. The input voltage, $f_2(t)$ ¹, is thus sampled at a delayed time, τ , by SAMPLER B. The output wave forms from SAMPLER A and B are compared in Figure 27.

Brief Review of τ -step Delay

N samples (a_N) are taken from $f_1(t)$ and (b_N) samples are taken from $f_2(t) = f_1(t)$, delayed τ seconds from a_N . The value of

¹ For autocorrelation $f_2(t) = f_1(t)$.

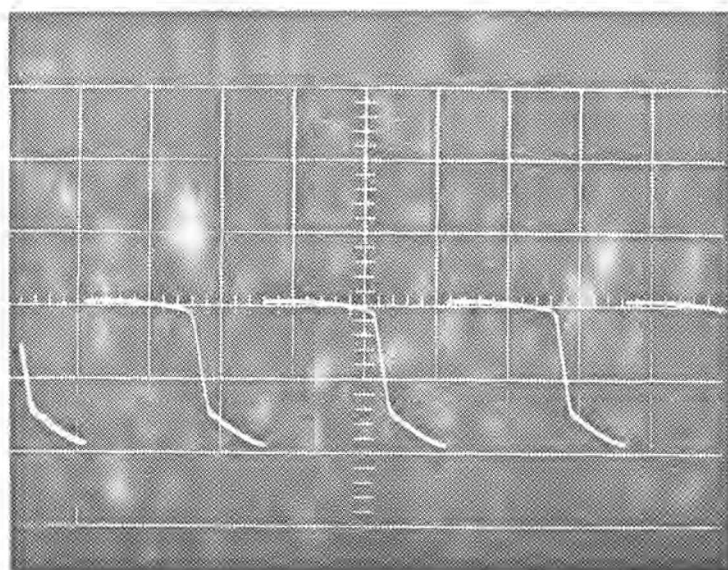
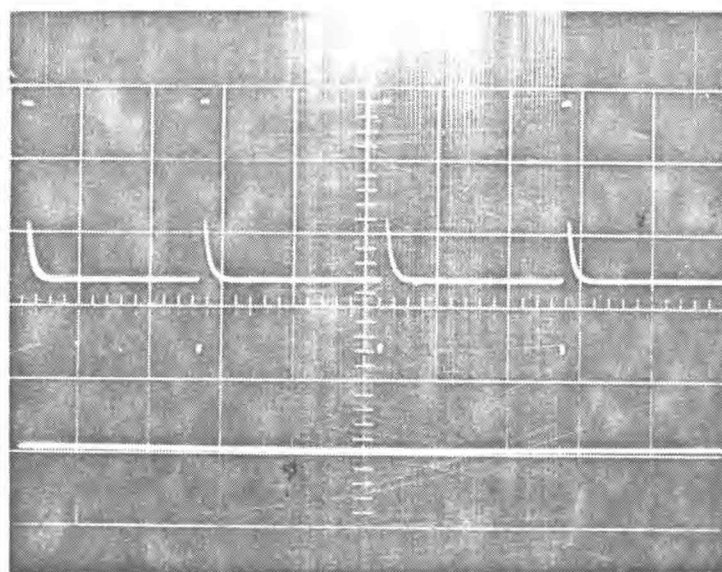


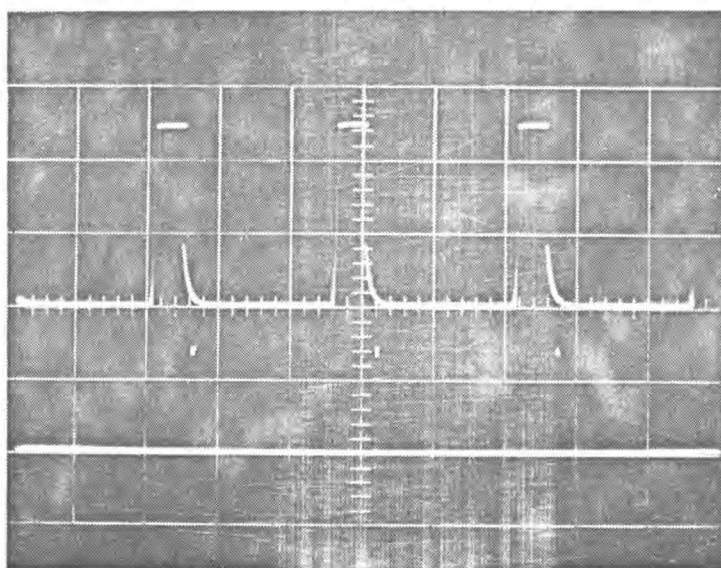
Figure 24. Schmitt trigger - 1 output voltage $T = 400 \mu\text{sec}$

Abscissa - 0.5 msec/cm

Ordinate - 1 volt/cm



(a)

Sampling Pulse
Train - a

(b)

Sampling Pulse
Train - a

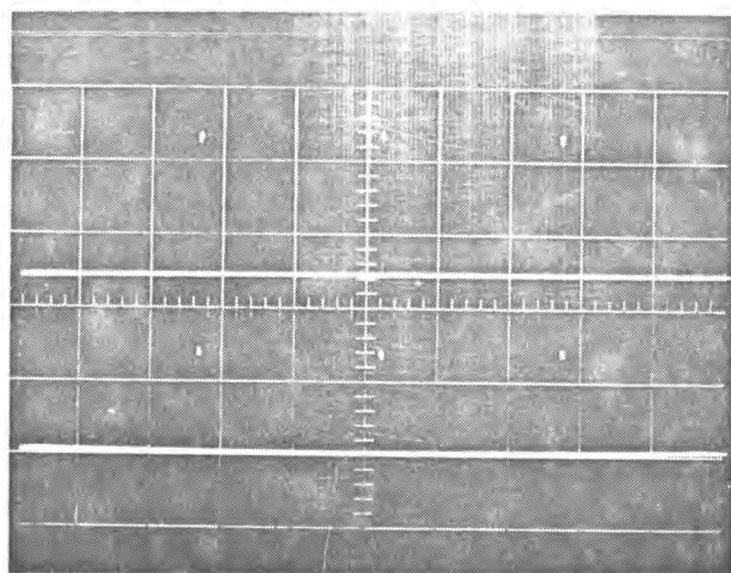
Figure 25. Schmitt trigger - 1 output voltage amplified by T_{21} .

Waveform (a) - No shift. Note how pulse rise is in phase with sampling pulse train - a.

Waveform (b) - 250 μ sec shift. Pulse rise has shifted 250 μ sec to the left of sampling pulse train - a.

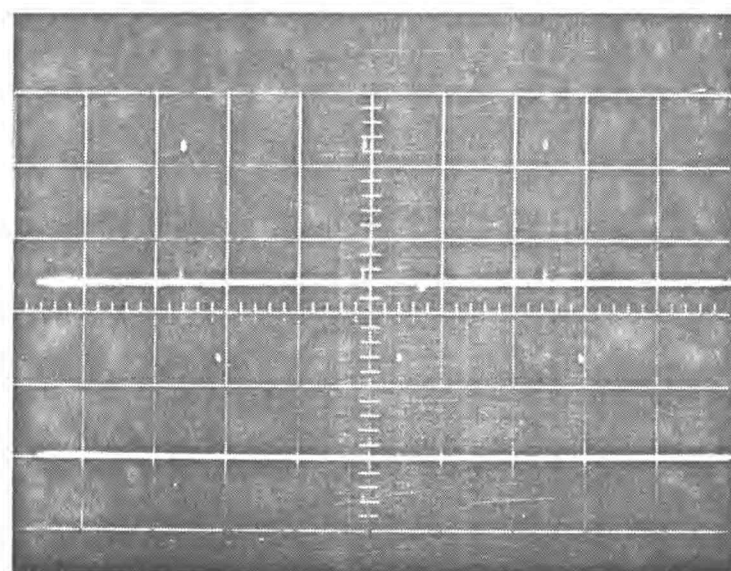
Abscissa - 0.5 msec/div

Ordinate - 5 v/div



Pulse train - b

Pulse train - a



Pulse train - b

Pulse train - a

Figure 26. Comparison of sampling pulse train a and b.

Top waveforms - No shift.

Bottom waveforms - 270 μ sec of shift

Abcissa - 0.5 msec/cm

Ordinate - 5 v/cm

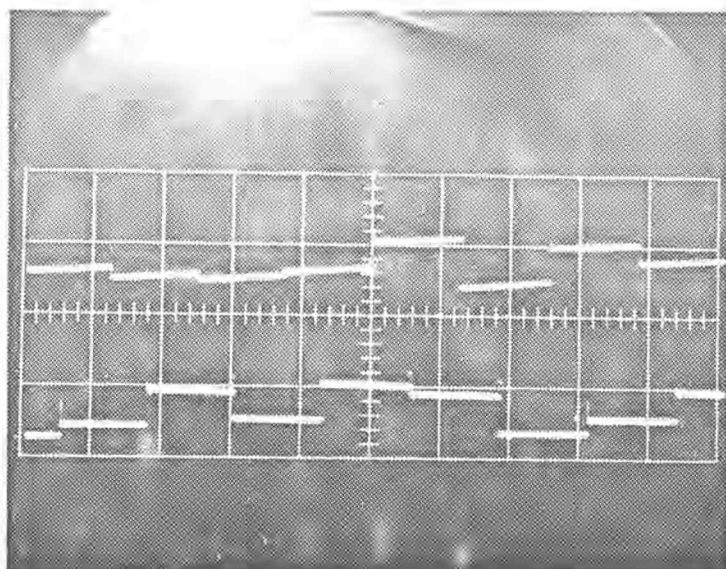


Figure 27. Comparison of sampler A and sampler B output waveforms.

Top waveform - Sample waveform of $f_1(t)$

Bottom waveform - Sample waveform of $f_2(t) = f_1(t + T)$

$T = 760 \mu\text{sec.}$ Abscissa - 1 msec/cm

Ordinate - 1 v/cm

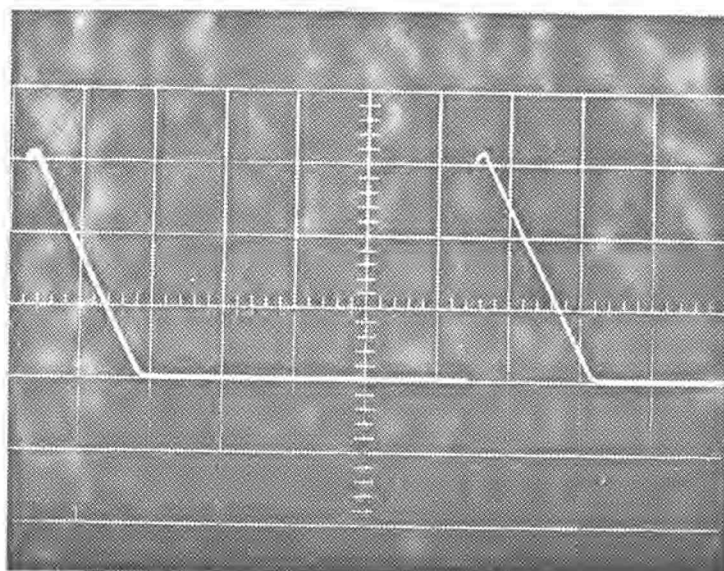


Figure 28. Miller sweep - 2 voltage.

Abcissa - $200 \mu\text{sec/cm}$

Ordinate - 2 v/cm

τ is then increased τ_k sec and N pairs (a_N, b_N) of samples are again taken. The shift in τ is negative (to the left), which corresponds to shifting $f_2(t)$ to the right. Shifting $f_1(t)$ to the left is not necessary since the autocorrelation function is even.

$$\text{i.e. } \phi_{11}(-\tau) = \phi_{11}(\tau)$$

Other Comments

It now becomes necessary to find

$a_1 b_1 + a_2 b_2 + \dots + a_i b_i + \dots + a_N b_N \cong \phi_{11}(\tau)$. This will be done by generating a pulse train with pulse amplitude equal to the values of a_i and width proportional to b_i . The resultant pulse train will be integrated and summed from $i = 1$ to N which will provide one point on the autocorrelation curve. A total of 220 pts are generated during 1 msec of shift. The total elapsed time is $(220 \text{ pts}) (5.33 \text{ sec/pt}) = 1170 \text{ seconds}$.

Pulse-Width Modulation

Schmitt trigger-2 is used to produce a pulse train with each pulse-width proportional to the corresponding value of b_i . The bias voltage for Schmitt trigger-2 is the output voltage from SAMPLER-B. The input voltage is the Miller sweep voltage shown in Figure 28.

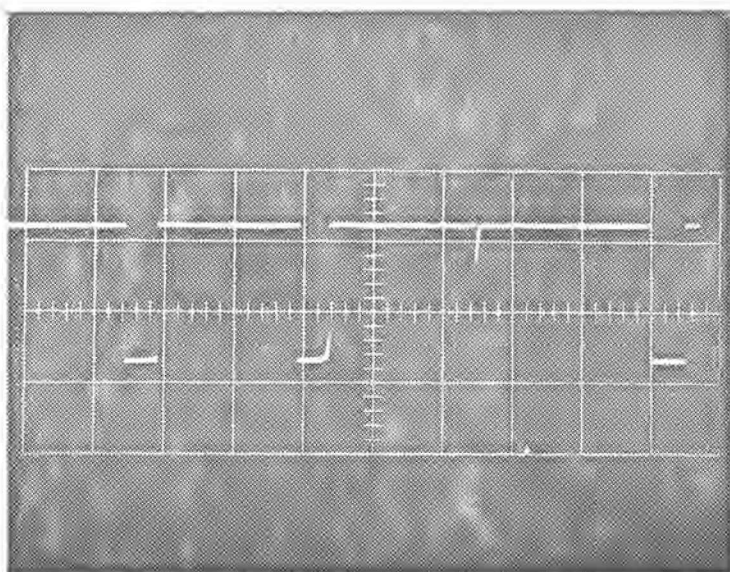


Figure 29. Pulse width modulated pulse train.

Abscissa - 0.5 msec/cm

Ordinate - 5 v/cm

The sweep voltage is clamped at zero volts and is coupled into the base of T_{33} . The bias voltage changes amplitude with each new sample, b_i . As explained earlier for Schmitt-trigger 1 the bias level determines the time required for switching to take place. The resulting waveform is a variable-width pulse train with the width of each pulse directly proportional to the bias voltage generated by SAMPLER-B output. The Schmitt-trigger output is amplified by T_{35} and the final result is shown in Figure 29.

Pulse-Height Modulation

The pulse-width modulated waveform and SAMPLER-A output are applied to the diode gate shown in Figure 30.

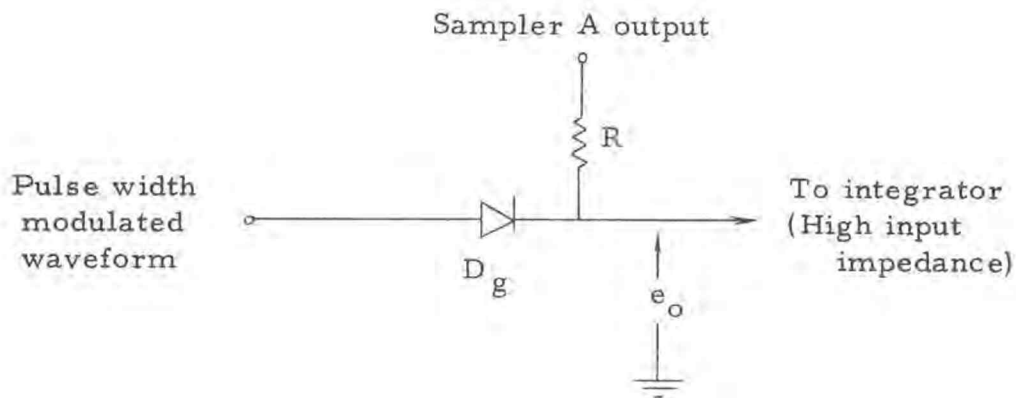


Figure 30. Diode gate.

When a pulse is applied to D_G it is reversed biased and becomes an open circuit ($2000 \text{ meg}\Omega$). The SAMPLER-A voltage appears at the gate output as long as it is coupled into a circuit whose input impedance is much greater than R . When the pulse is removed D_G is forward biased and assumes a very low impedance. The pulse width modulator output resistance, R_o , is very low when not producing a pulse. The value of $R_o + R_f$ is much less than R so SAMPLER-A voltage is dropped across R and the value of e_{out} is zero. The resulting waveform is shown in Figure 31. The height of each pulse is equal to a_i and width is proportional to b_i .

Integrator-Summer

There are 4096 of the above pulses generated for each value of T . These pulses are integrated by an operational amplifier (O. A.). The O. A. output voltage increases an amount proportional to the area of each pulse; each area being equal to $a_1 b_1, a_2 b_2, \dots, a_N b_N$. The O. A. holds the value of each successive integration and the output voltage is thus equal to

$$a_1 b_1 + a_2 b_2 + a_3 b_3 + \dots + a_N b_N = \sum_{i=1}^N a_i b_i$$

After N pairs of samples (a_N, b_N) have been integrated and summed the integrator is reset to zero volts, T is increased T_k

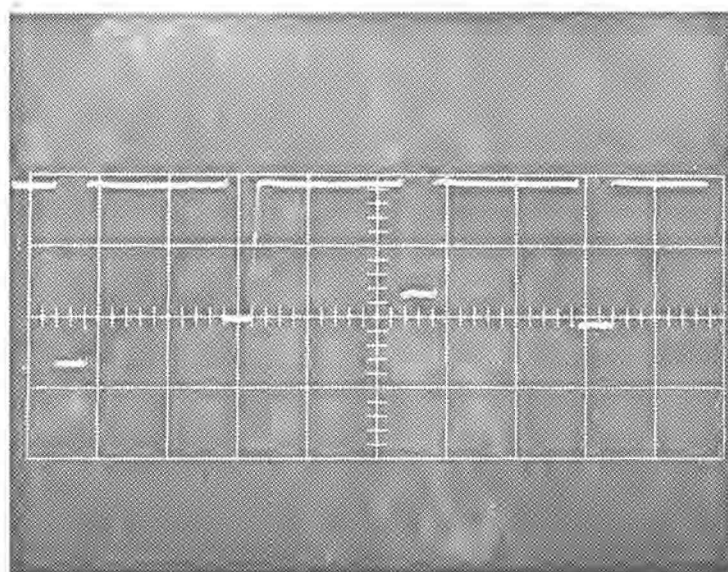


Figure 31. Pulse width and height modulated pulse train.

Abscissa - 0.5 msec/cm

Ordinate - 2 volt/cm

seconds, and the process is repeated.

The discharge time constant of the integrator capacitor should be large compared to the total time consumed in computing one point of the correlation curve. The time constant seen by the integrator capacitor is 2000 seconds. The computation time is 5.33 seconds for 4096 sample at a 750 cps rate, therefore little discharge will occur.

Read Out

The integrator output voltage is monitored by a strip chart recorder was used to obtain data for this thesis. Any recorder with sensitivity of 0.1v, frequency response of 100 cps, and zero suppression can be used.

Integrator Reset Circuit

The integrator is reset to zero volts by an electro-mechanical switch as shown in Figure 32. The coil is activated the same instant is increased. The pulse shaping network provides a pulse of sufficient width (0.1 sec) to cause switching. The bias voltage, E , for T_{44} must be greater than 20 volts to activate the coil when T_{44} is switched on. A short circuit from the integrator capacitor to ground discharges C instantaneously.

This completes the discussion of the system and its operation. How well the system will correlate and detect a periodic signal in

random noise is the next question. Extensive tests were run to determine the quality of operation and limitations of the design. These results and answers to the above questions are now presented.

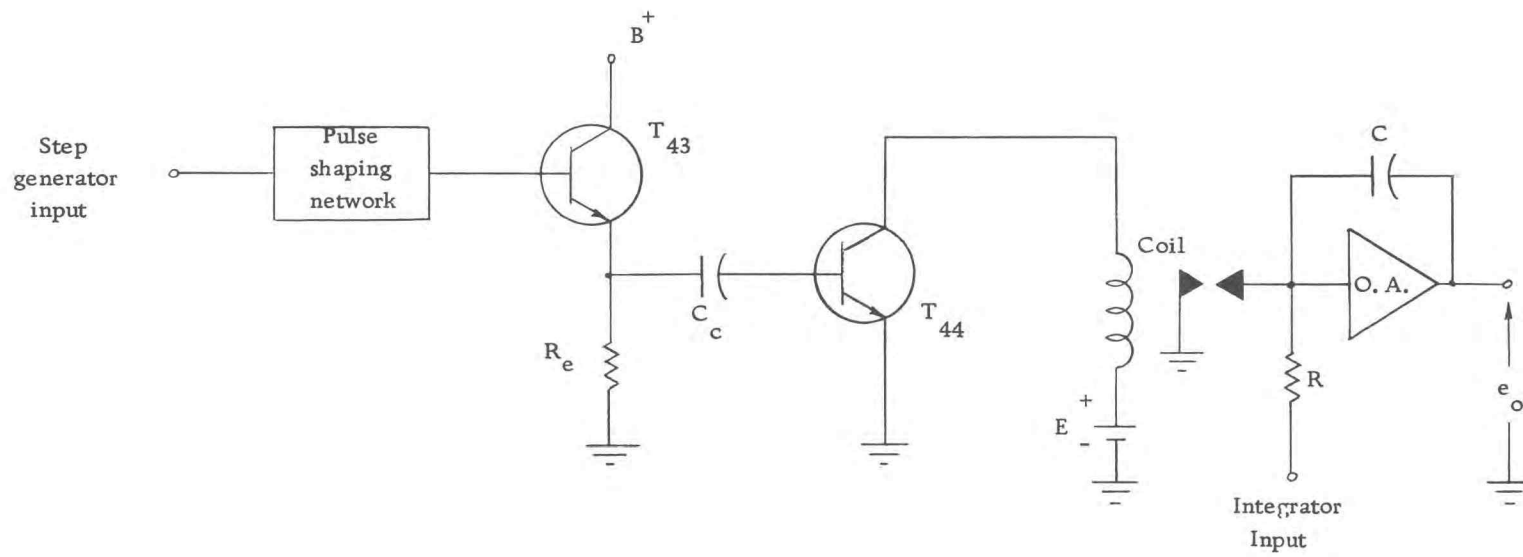


Figure 32. Integrator reset circuit.

SYSTEM EVALUATION

To evaluate any system the theoretical, or expected quality of operation, must be compared to the actual results obtained from the system. The present section of the thesis will discuss the expected results first and then compare this to actual data taken from the correlator.

Frequency Response

The autocorrelation of a periodic sinusoid with frequency f_1 is shown in Figure 33. The peak value of each spike traces out a

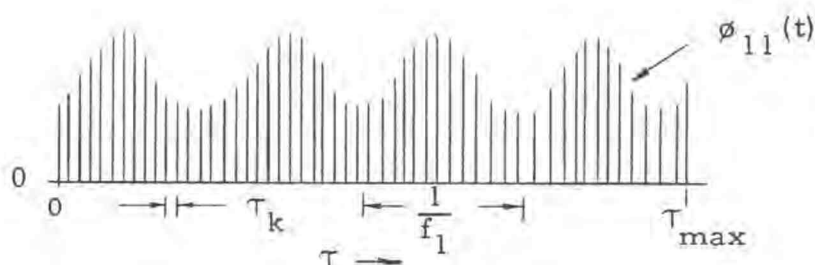


Figure 33. Autocorrelation of periodic sinusoid, $f_1(t)$.

sinusoid with exactly the same frequency as the input signal, $f_1(t)$. The d. c. level was introduced at the input and consequently will appear at the output.

The peak-peak value of $\phi_{11}(\tau)$ is proportional to the peak-peak value of $f_1(t)$. The proportionality constant would be very

difficult to compute for such an elaborate system and is not important. The purpose of autocorrelation is to determine the following two things.

1. Is there a periodic signal present in the time function being correlated?
2. What is the frequency of the periodic signal?

By observing the correlator output the above two questions can be answered.

In Figure 33 there are 14 points tracing out each cycle of $\phi_{11}(\tau)$, and the points are τ_k seconds apart. The number of points per cycle determines the readability and accuracy of $\phi_{11}(\tau)$. If the value of τ_k is $5\mu\text{sec}$, and the input frequency is 10kc, $\phi_{11}(\tau)$ will contain 20 points/cycle. If the input frequency is increased to 40kc only 5 pts/cycle appear at the output, which is inadequate for determining the frequency of $\phi_{11}(\tau)$. This can best be illustrated by the sequence of possible output waveforms for $\phi_{11}(\tau)$ shown in Figure 34.

The readability of the 5kc signal is good, as is the 10kc and 20kc waveform. For the 40kc signal only 5 pts/cycle are present which is not enough for accurate reproduction. If the value of τ_k were reduced to $2.5\mu\text{sec}$ then the 40kc signal would be as readable as the 20kc signal. This introduces the problem of how small to make τ_k . The main problem arises in the lower

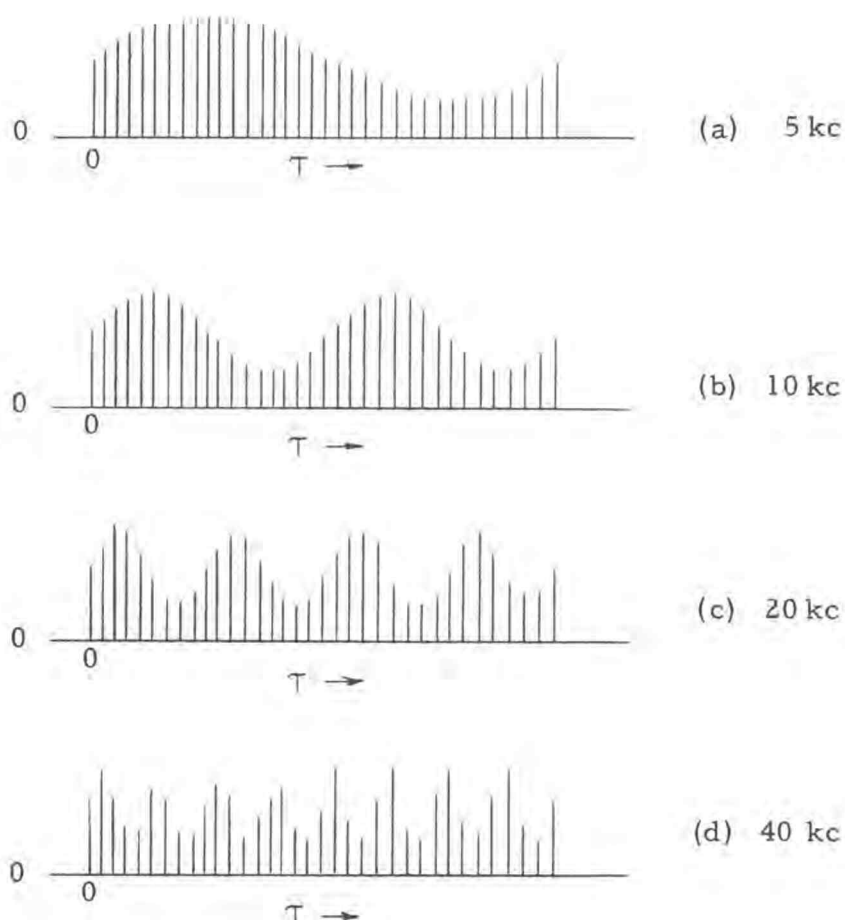


Figure 34. Possible frequency response of correlator with $\tau_k = 5 \mu\text{sec}$.

frequency limit is set at 2kc, and the total shift in τ is 1 msec. The average value of τ_k is made equal to $4.55 \mu\text{sec}$ so it will take 220 pts, or discrete steps of τ_k , to shift 1 msec. The correlator takes 4096 samples at each discrete step at a rate of 750 samples/second. The resulting time required to correlate two cycles of a 2kc signal is 1200 seconds or 20 minutes. This value of τ_k would limit the upper frequency to approximately 30kc. If τ_k

were reduced to $2.25\mu\text{sec}$ the upper frequency limit would become 60kc, but the time required to autocorrelate a 2kc signal would increase to 40 minutes.

The time required to shift $f_1(t+\tau)$ with respect to $f_1(t)$ is dependent on three things.

1. The value of τ_k .
2. The number, N , of sample pairs taken.
3. The total shift, τ , required.

The average value of τ_k is given since its value decreases in an exponential fashion as shown in Figure 35. The straight line shows the relationship between the amount of shift, τ , and the number of discrete steps, τ_k , required to produce τ for a linear system. The curved line was taken from experimental data and shows the actual number of discrete steps, τ_k , required to produce a shift of τ seconds.

The complete frequency spectrum of the correlator is shown in Figure 36-40. Notice the exponential increase in the number of pts/cycle as τ becomes larger. The number of points required to trace out each additional cycle is greater than the previous cycle.

Assume for the present the input frequency of $f_1(t)$ is not known. To determine this frequency from $\phi_{11}(\tau)$ the following procedure is used in conjunction with Figure 35.

1. The horizontal time axis for all data is

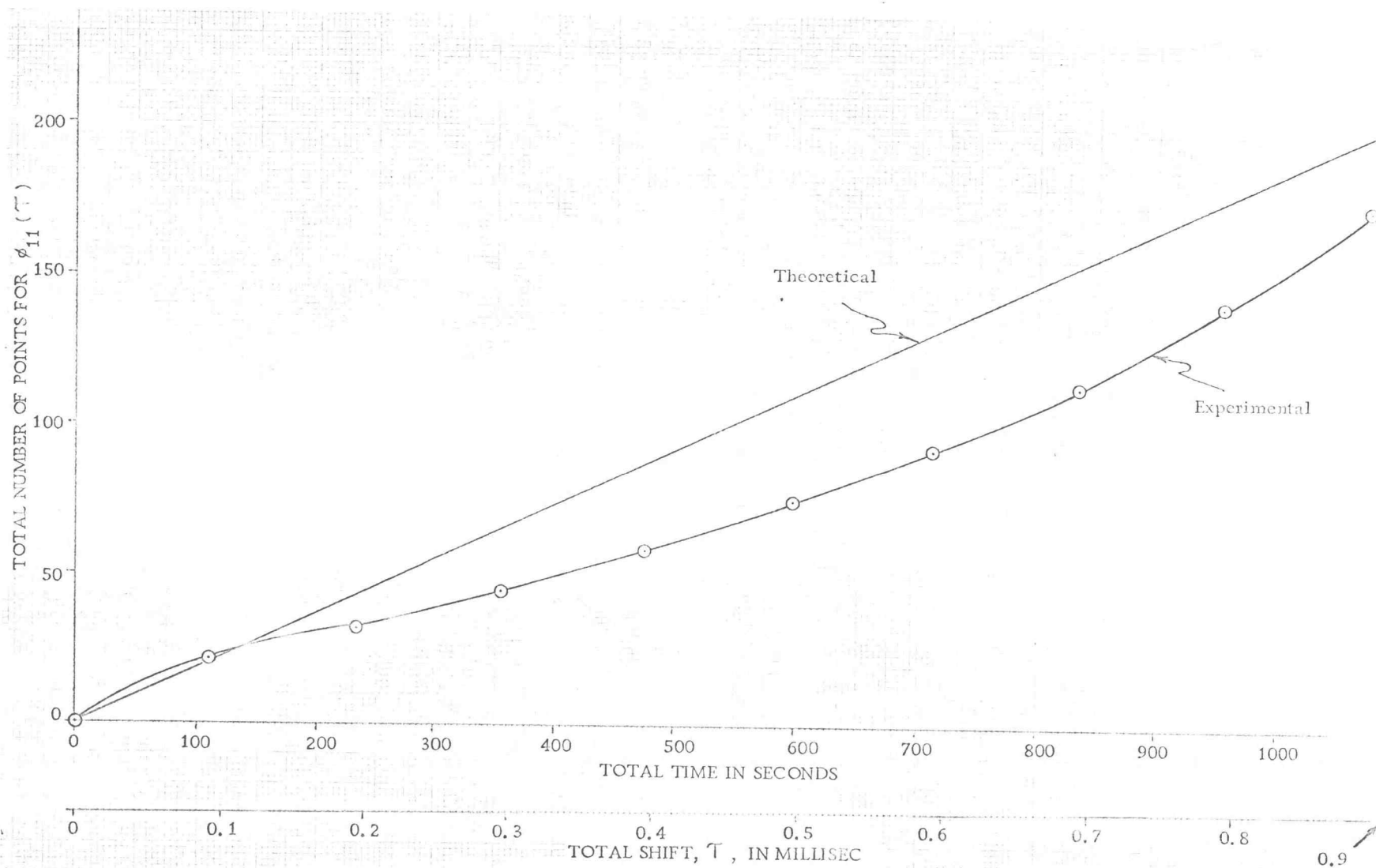


Figure 35. Relationship between time taken for τ shift and actual value of τ on horizontal axis, vs number of points produced on correlation curve for τ shift.

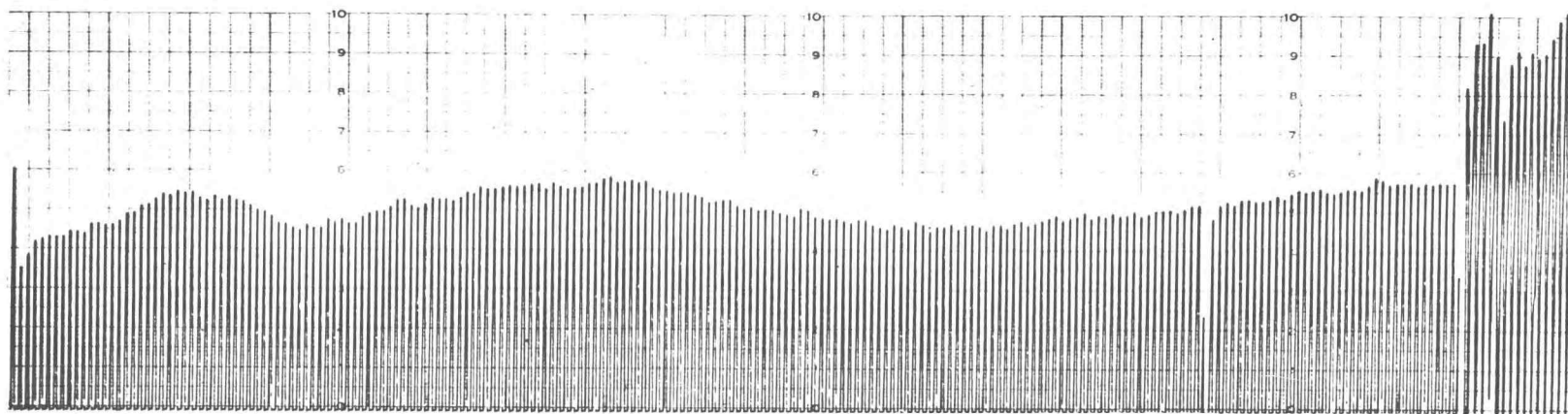


Figure 36. Autocorrelation of 2kc sinusoid. No noise. Vertical - 50m volts/division. Horizontal - 18sec/division.

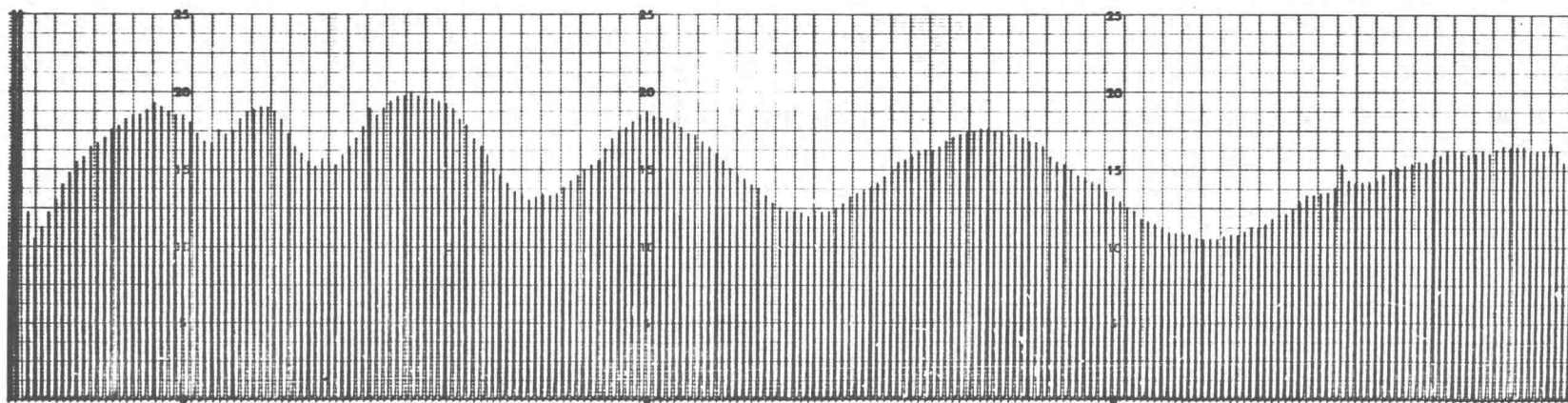


Figure 37. Autocorrelation of 5kc sinusoid. No noise. Vertical - 50m volts/division. Horizontal - 18sec/division.

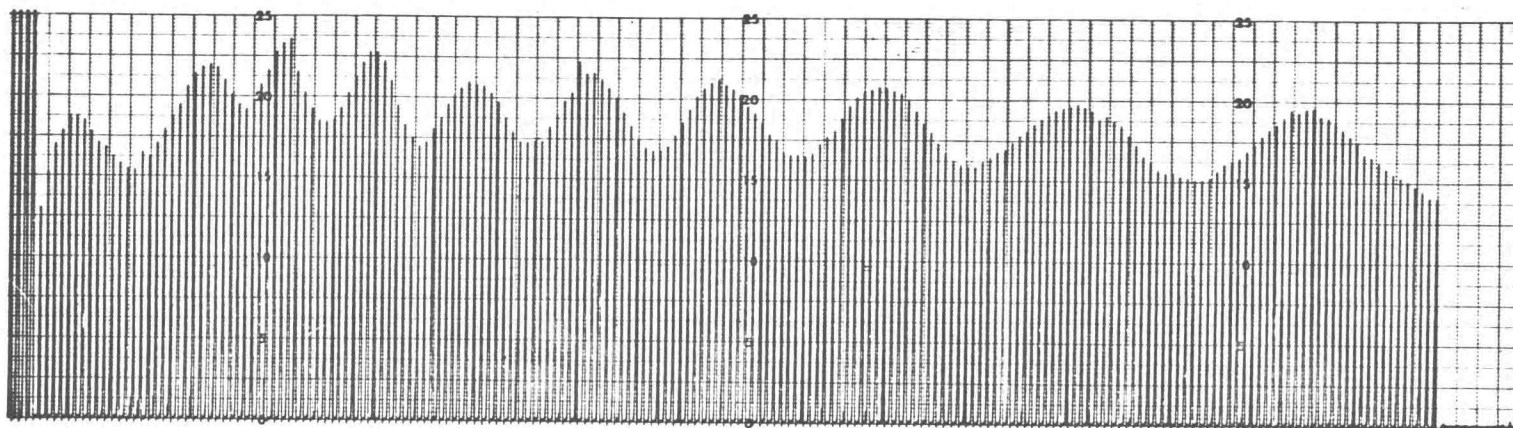


Figure 38. Autocorrelation of 10kc sinusoid. No noise. Vertical - 50m volts/division. Horizontal - 18sec/division.

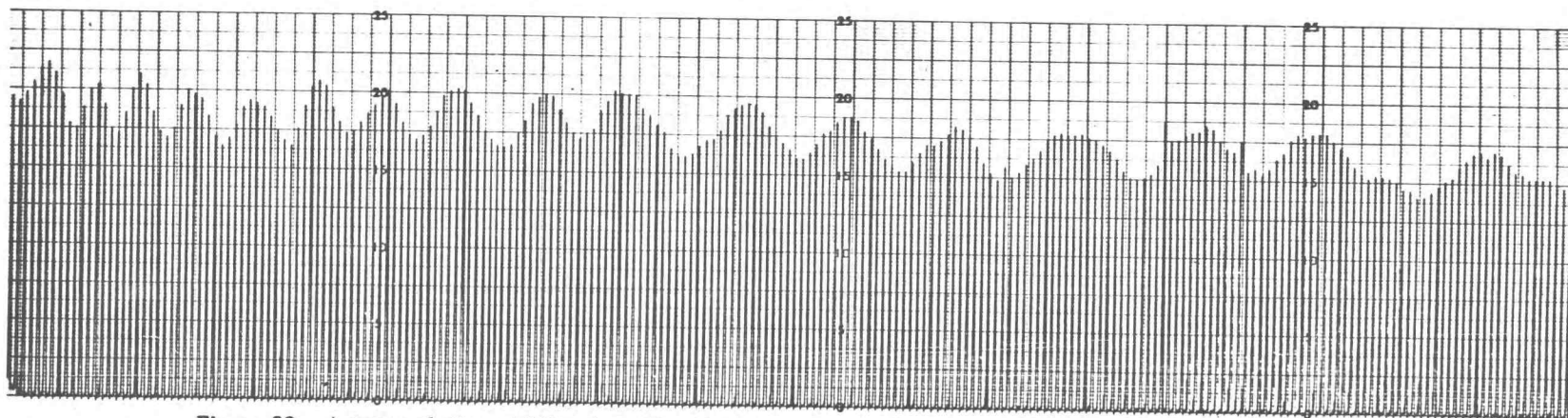


Figure 39. Autocorrelation of 20kc sinusoid. No noise. Vertical - 50m volts/division. Horizontal - 18sec/division.

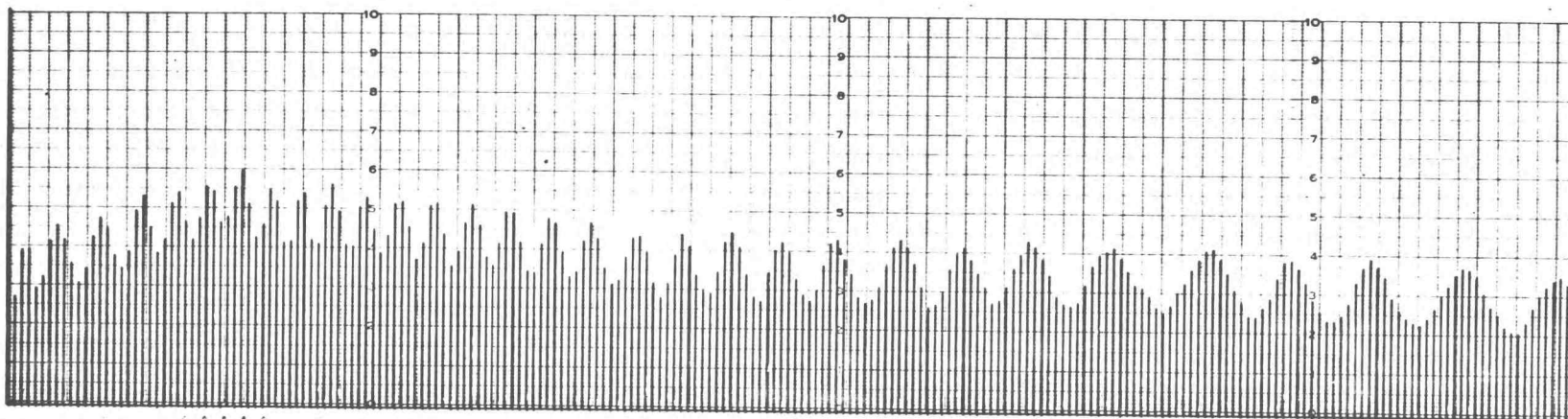


Figure 40. Autocorrelation of 30kc sinusoid. No noise. Vertical - 50m volts/division. Horizontal - 18sec/division.

18 sec/division. Starting with the first amplitude peak determine the time elapsed from t_1 to any n^{th} cycle. The time value $(t_n - t_1)$ will be ΔT .

2. Determine from vertical axis in Figure 35 the experimental and theoretical number of points on the correlation curve from t_1 to t_n .

$$R = \frac{\text{Theoretical Number}}{\text{Experimental Number}}$$

3. Determine the change in shift, ΔT , corresponding to ΔT .
4. The time of n cycles will be $(R) (\Delta T)$.

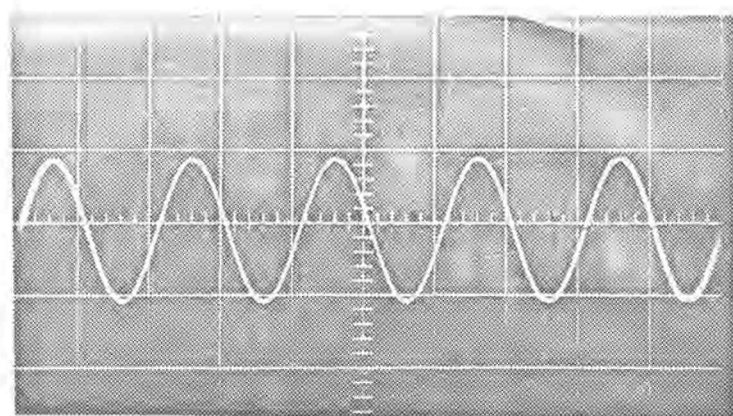
The frequency of the input signal will be

$$f = \frac{n}{(R) (\Delta T)}$$

Noise Response

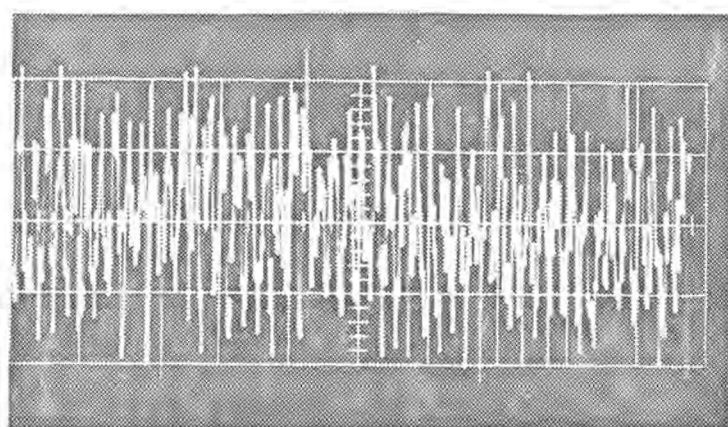
The most important function of the correlator, and primary purpose for its design, is to detect periodic signals in random noise.

Figure 41 shows a 10kc periodic signal summed with an



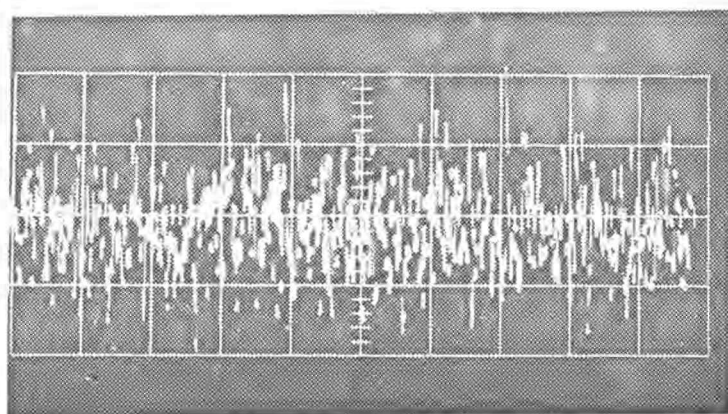
(a)

10 kc signal.
 No noise.
 Abscissa -
 0.5 msec/cm
 Ordinate - 0.5 v/cm



(b)

10 kc signal + noise.
 $N/S = 0$ db
 $N/S = 6$ db¹
 Abscissa -
 0.5 msec/cm
 Ordinate - 0.5 v/cm



(c)

10 kc signal + noise.
 $N/S = 10$ db
 $N/S = 16.8$ db
 Abscissa -
 0.5 msec/cm
 Ordinate - 2 v/cm

Figure 41. Distortion of sinusoid by addition of noise.

¹ Noise and signal in peak-peak values.

The rms value of random noise is defined (7, p. 73) as the standard deviation, σ , of its PDF. A peak value of 2 volts for random noise would have an rms value of ≈ 0.4 volts. Sixty-eight per cent of the time the noise level will fall in the interval $(-0.4 < v < 0.4)$ and the remainder of the time outside this interval.

The sum of noise + signal at the input must be kept ≤ 7 volts pk-pk, or error will result in sampling as mentioned when discussing the system operation (p. 30). It is also necessary to have at least 0.4 rms volts of periodic signal at the input. This is to provide 0.3 to 0.4 pk-pk volts for $\phi_{11}(T)$.

A N/S ratio of 10db ($S = 0.4$ rms volts, $N = 1.3$ rms volts) is shown in Figure 43(c). Note that the pk-pk value of this input signal is approximately 7 volts, with the heaviest concentration between ± 2 volts.

The autocorrelation of periodic sinusoids with various N/S ratios are shown on the following pages. Figures 43-46 show the result for autocorrelation of a 10kc signal with N/S ratio from 0 to 10 db. Deviation from a perfect sinusoid at the output is considered output noise. When the input N/S is less than 5db there is no appreciable output noise, and the frequency of the sinusoid can easily be calculated. At A N/S level of 10db there is considerable output noise but the periodic signal amplitude is well above the noise level. This is the largest N/S ratio that can be tested by the correlator due to limitations on pk-pk values of input voltage as already mentioned. Figure 49-54 show the frequency response of the correlator with large amounts of input noise.

As mentioned earlier there is noise present in the correlator

output. If this noise could be measured the overall S/N gain could be calculated. It would be very difficult, however, to determine the amount of output noise from the strip chart recorded data. If the output data could be converted to an electrical signal the frequency spectrum could be determined. All frequencies present in the output other than the known periodic component would be noise. If the N/S ratio at the output were -10db, which is a very reasonable figure, the overall system gain is 20db (input N/S = 10db). To further increase the system gain more samples could be taken. There are 4096 being taken in this correlator, and the literature (6) has mention of 16,000 samples used to average the output noise to zero. As mentioned earlier the number, N, is limited to 4096 to avoid an excessive length of time for correlation. The system is working quite well for the relatively small number of samples being taken.

Some of the output data will be difficult to interpret. It is therefore important that an experienced observer, who knows what to look for, analyze the data. He should be completely familiar with the correlators operation under normal conditions, and the limitations of the system.

Periodic Pulse Train Detection in Noise

The theoretical autocorrelation function for a periodic waveform of rectangular pulses is shown in Figure 55.

The two waveforms in Figure 56 show $f_1(t)$ with no noise

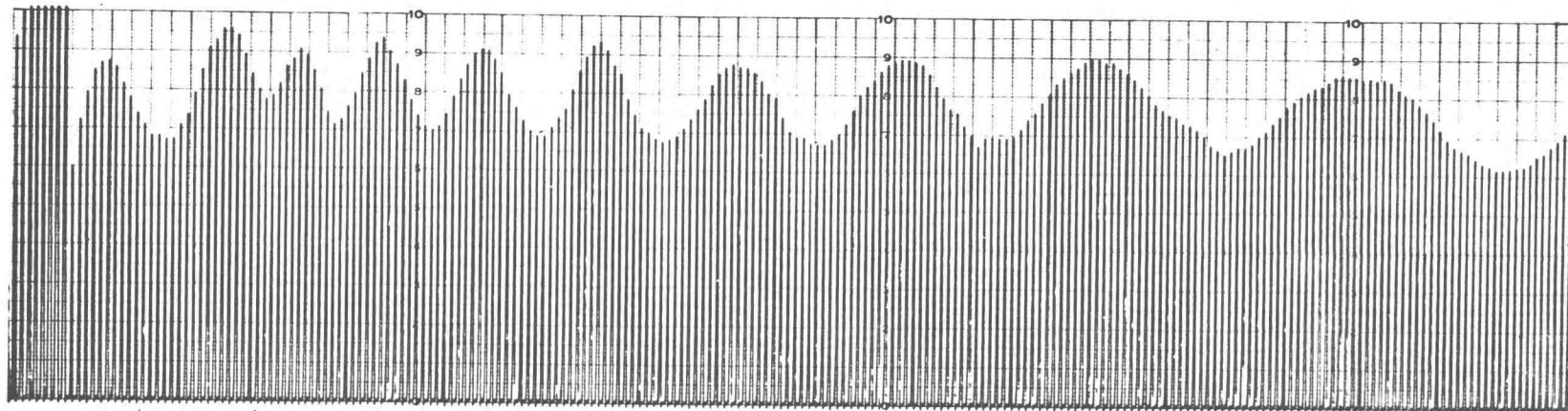


Figure 43. Autocorrelation of 10kc sinusoid. No noise. Vertical - 50m volts/division. Horizontal - 18sec/division.

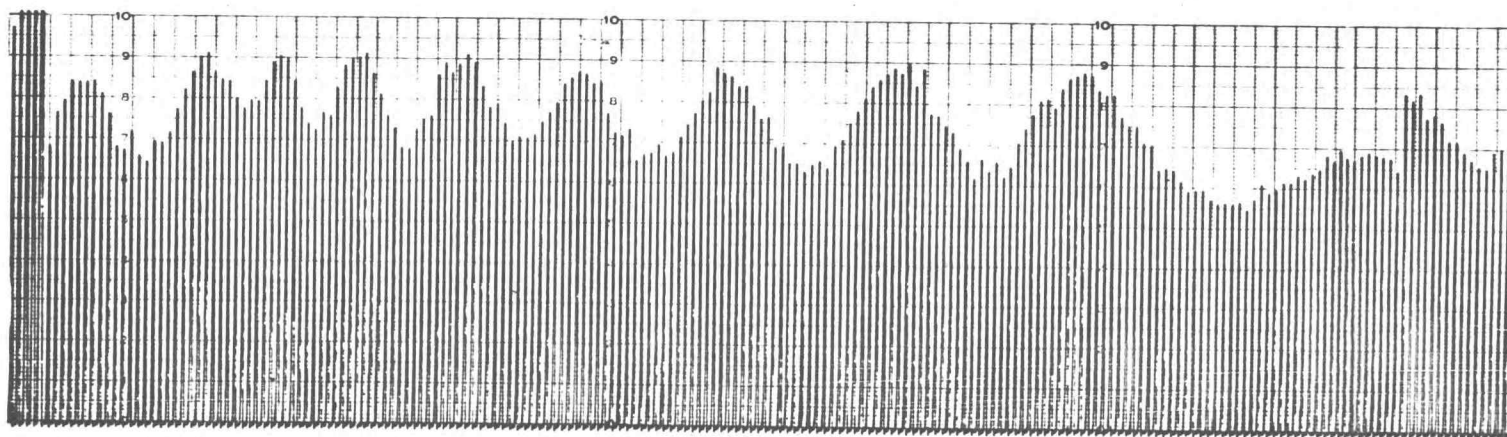


Figure 44. Autocorrelation of 10kc sinusoid + noise. N/S ratio 0db. Vertical - 50m volts/division. Horizontal - 18sec/division.

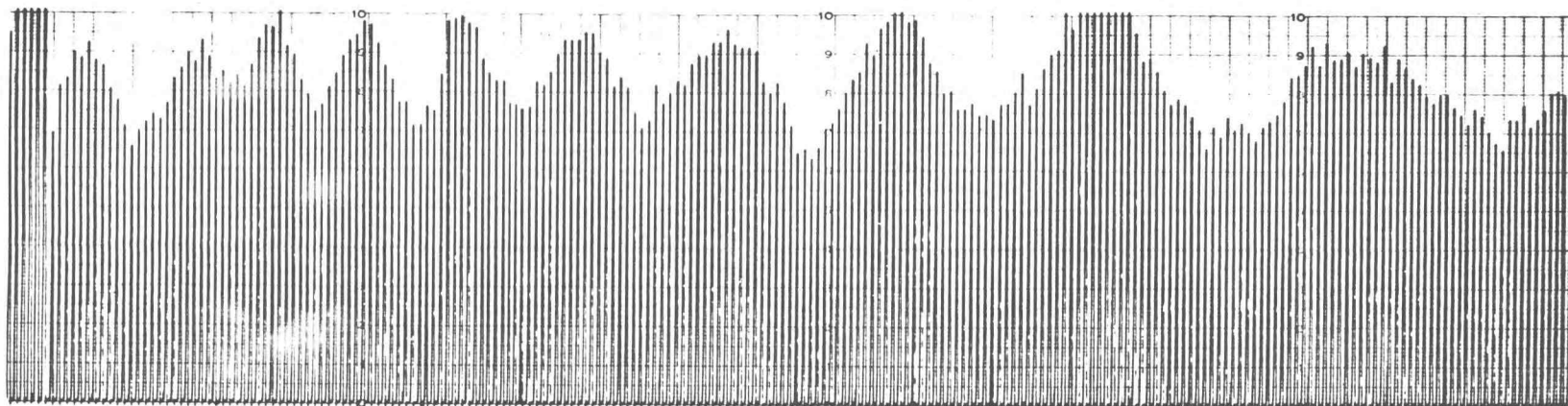


Figure 45. Autocorrelation of 10kc signal + noise. N/S ratio 2db. Vertical - 50m volts/division. Horizontal - 18sec/division.

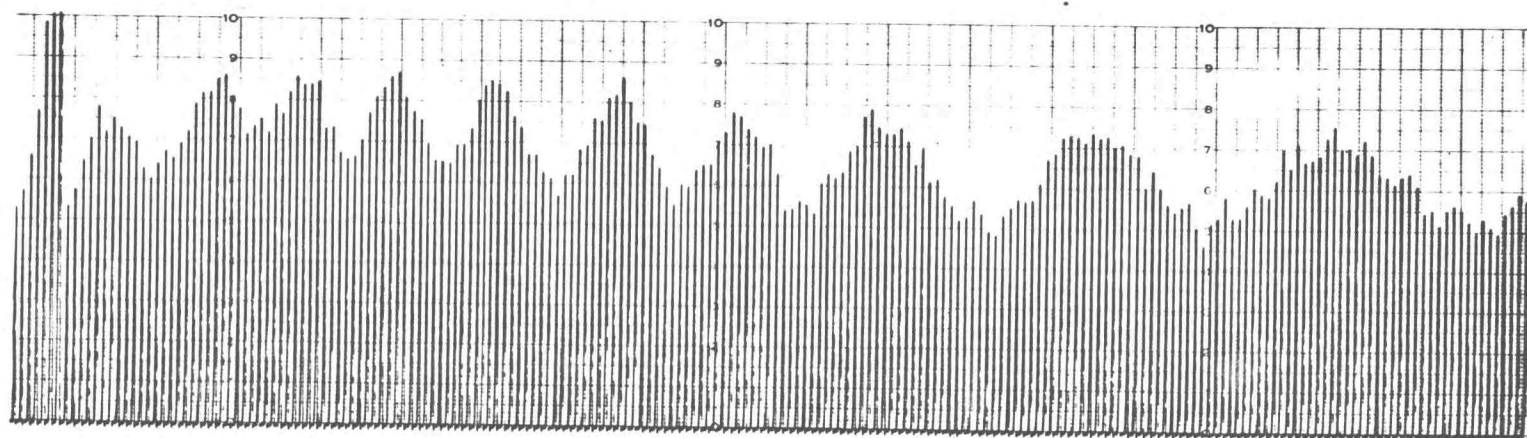


Figure 46. Autocorrelation of 10kc signal + noise. N/S ratio 5db. Vertical - 50m volts/division. Horizontal - 18sec/division.

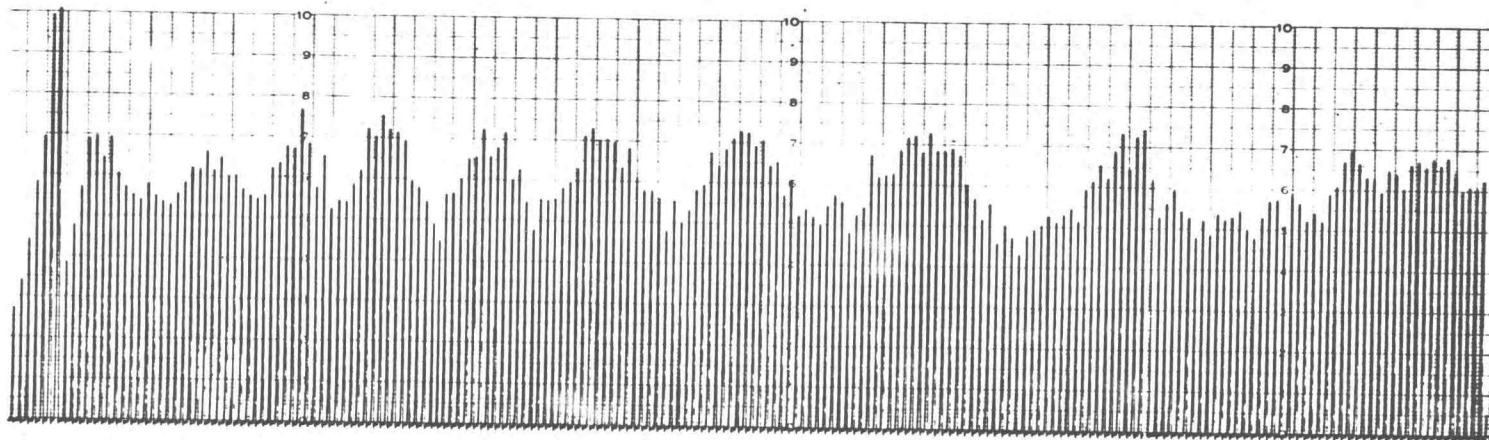


Figure 47. Autocorrelation of 10kc signal + noise. N/S ratio 7.5db. Vertical - 50m volts/division. Horizontal - 18sec/division.

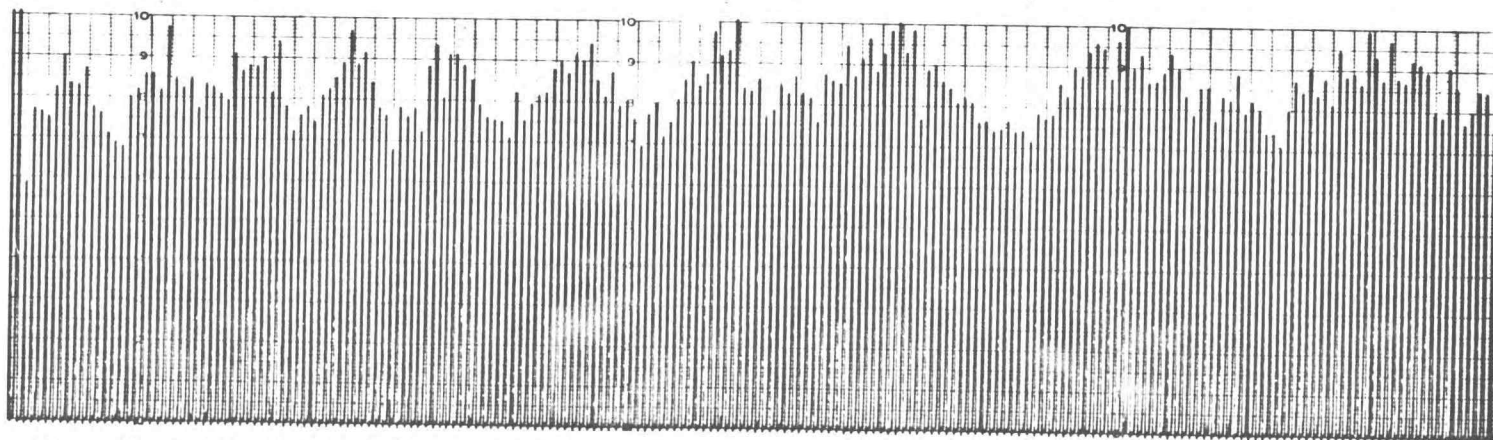


Figure 48. Autocorrelation of 10kc signal + noise. N/S ratio 10db. Vertical - 50m volts/division. Horizontal - 18sec/division.

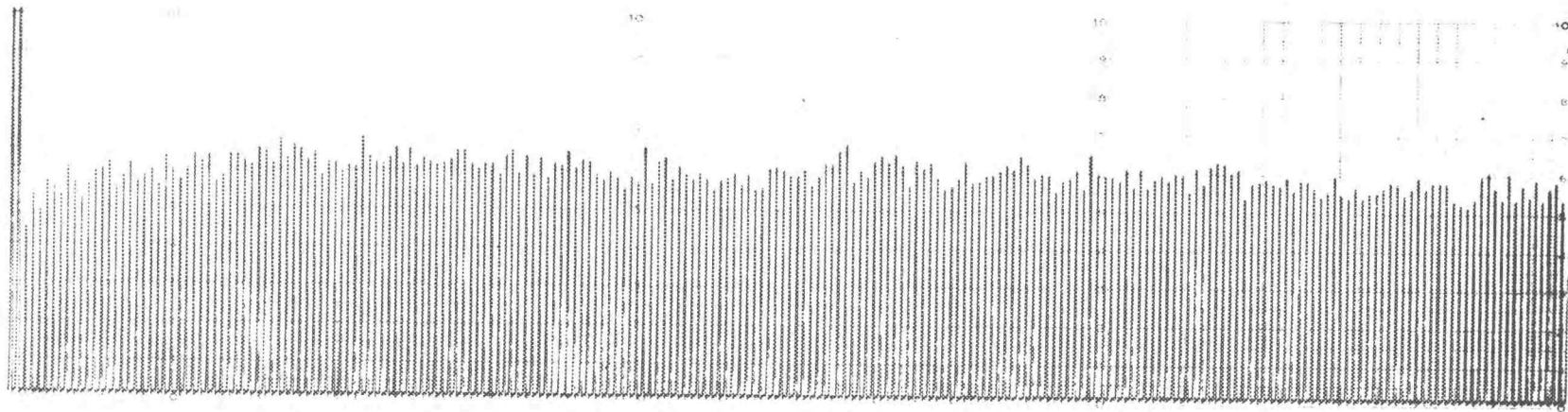


Figure 49. Autocorrelation of noise. No signal. Vertical - 50m volts/division. Horizontal - 18sec/division.

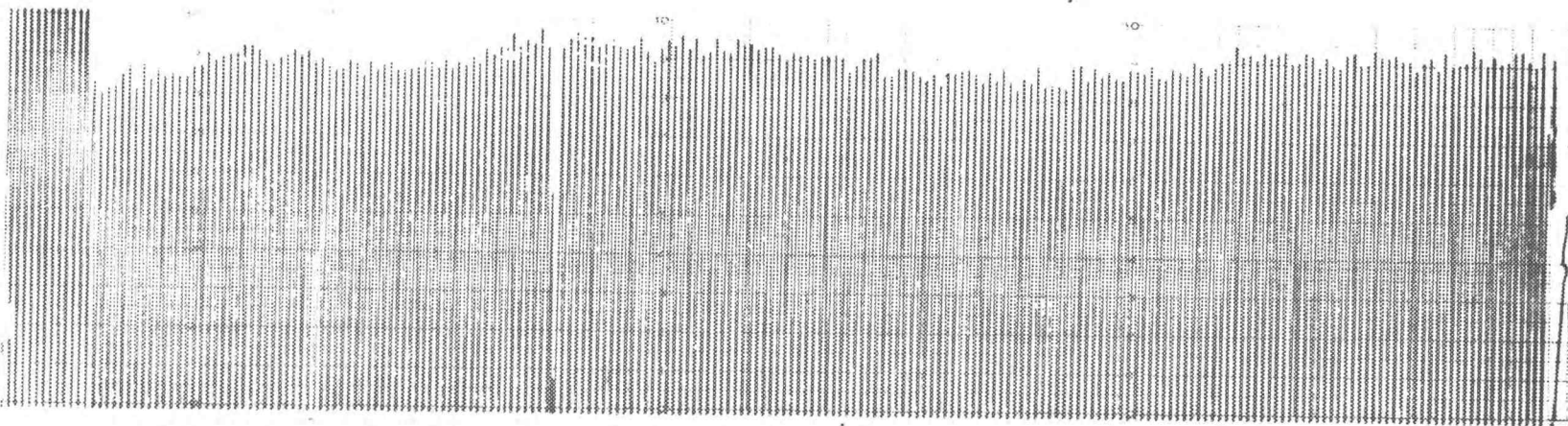


Figure 50. Autocorrelation of 2kc signal + noise. N/S = 10db. Vertical - 50m volts/division. Horizontal - 18sec/division.

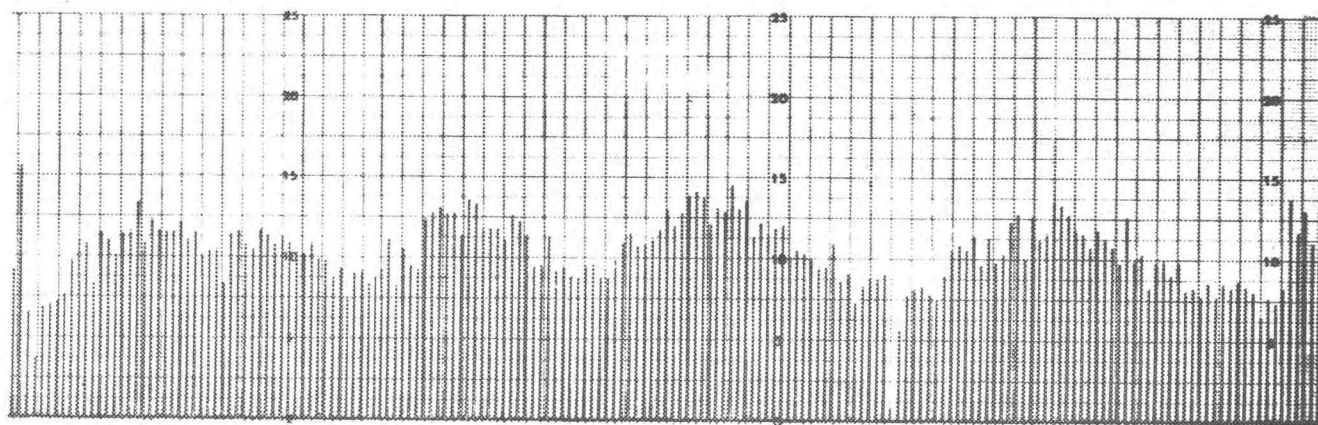


Figure 51. Autocorrelation of 5kc signal + noise. N/S ratio = 10db. Vertical - 50m volts/division. Horizontal - 18sec/division.

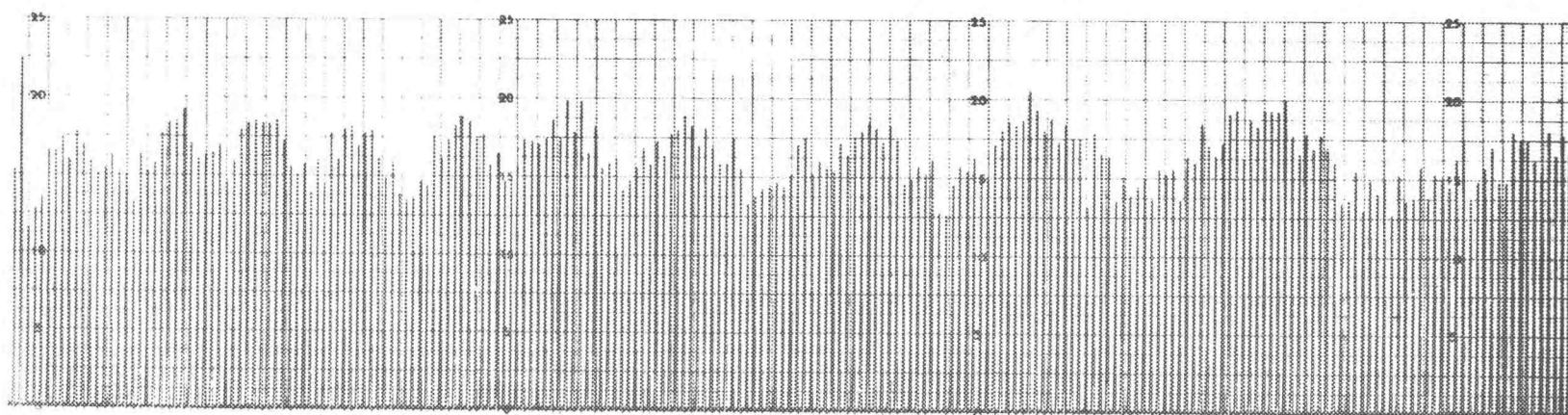


Figure 52. Autocorrelation of 10kc signal + noise. N/S ratio = 10db. Vertical - 50m volts/division. Horizontal - 18sec/division.

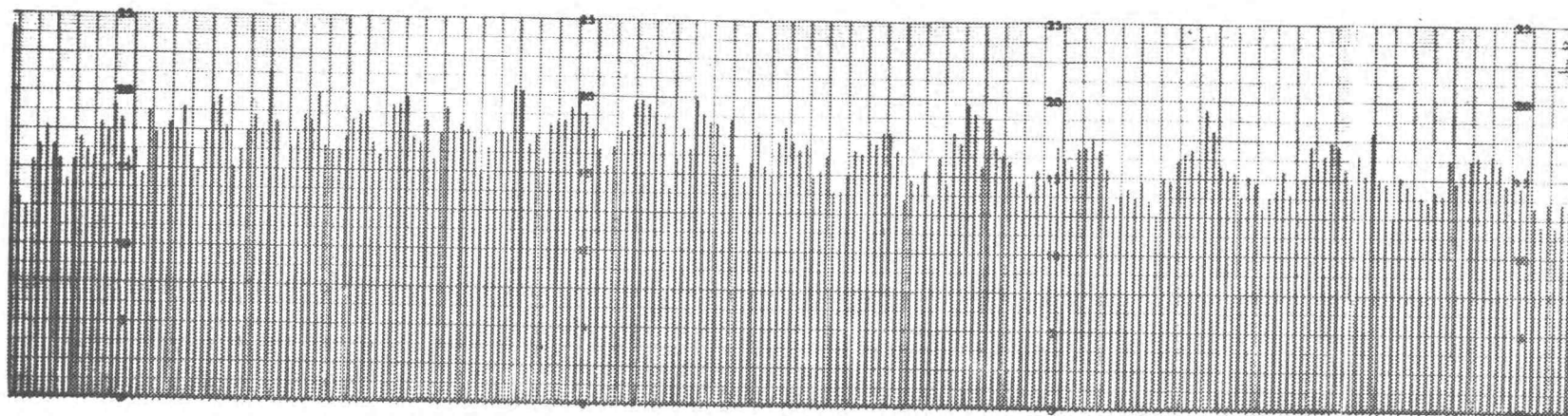


Figure 53. Autocorrelation of 20kc signal + noise. N/S ratio = 10db. Vertical - 50m volts/division. Horizontal - 18sec/division.

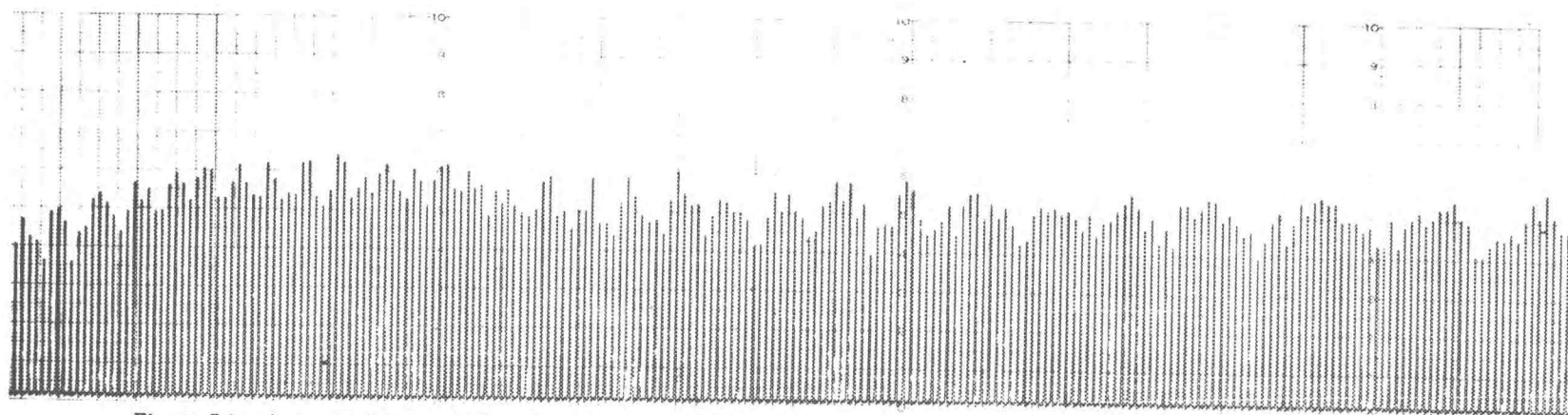


Figure 54. Autocorrelation of 30kc signal + noise. N/S = 10db. Vertical - 50m volts/division. Horizontal - 18sec/division.

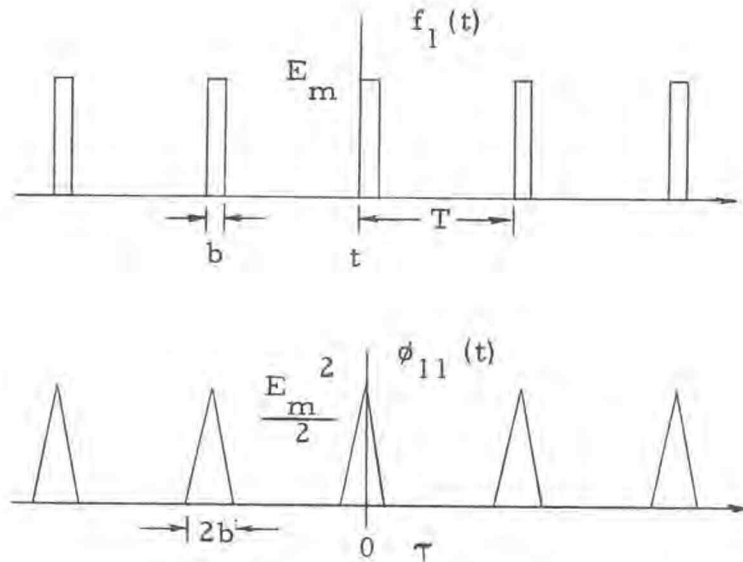


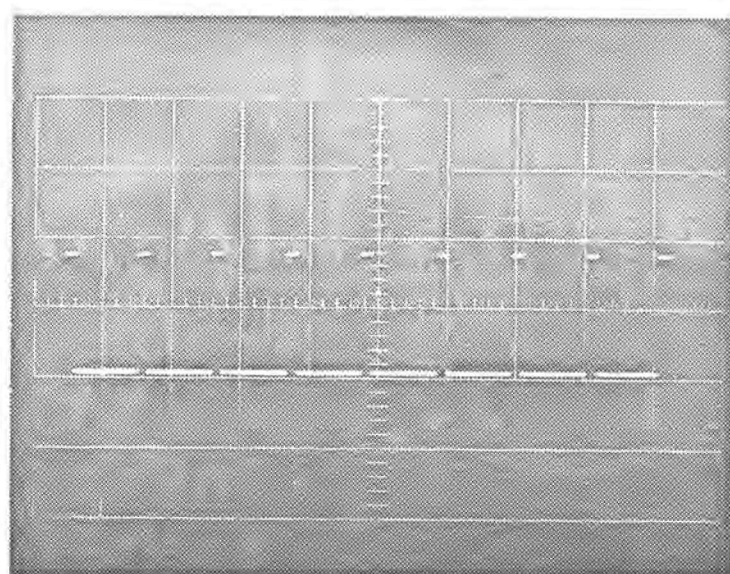
Figure 55. Autocorrelation function for periodic pulse train.

and summed with 1 vrms of noise. The autocorrelation function of these waveforms is shown in Figure 57. Note that $\phi_{11}(\tau)$ is inverted and superimposed on a d.c. level. The d.c. level was introduced at the input. Polarity inversion is due to sampling $f_1(t)$ when positive and then converting the samples to negative values and amplifying with p-n-p transistors.

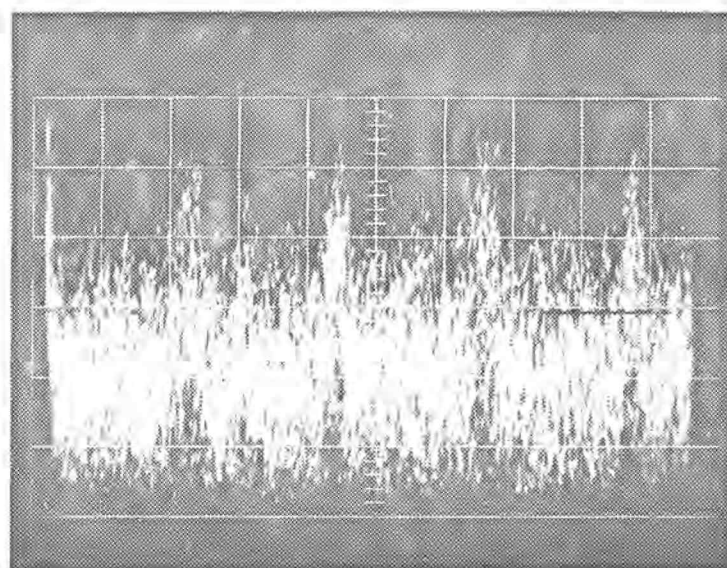
The autocorrelation of Figure 56(b) has considerable noise in the output, but the triangular pulses are still evident.

It should be noted that the apparent pulse rate in Figure 56(b) and the actual pulse repetition rate in 56(a) are not the same.

Application of correlation to transmission and communication lines could have considerable importance in detection of line faults.



(a)



(b)

Figure 56. Distortion of pulse train by addition of random noise.

Waveform (a) - No noise. Pulse train only.

Waveform (b) - $1v_{rms}$ noise + pulse train.

Abcissa - $200\mu\text{sec/cm}$

Ordinate - 1 volt/cm

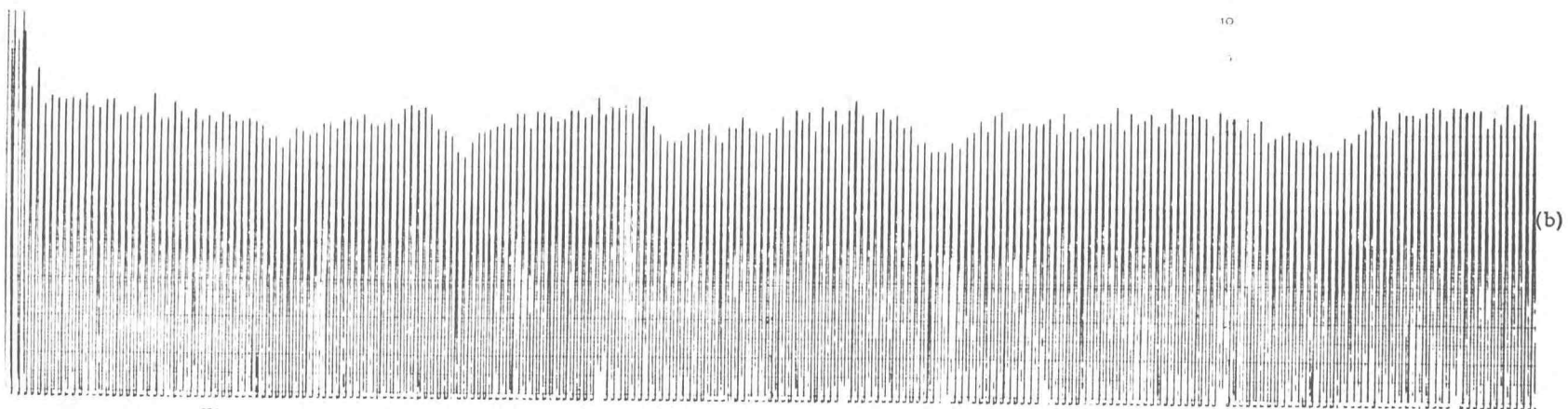
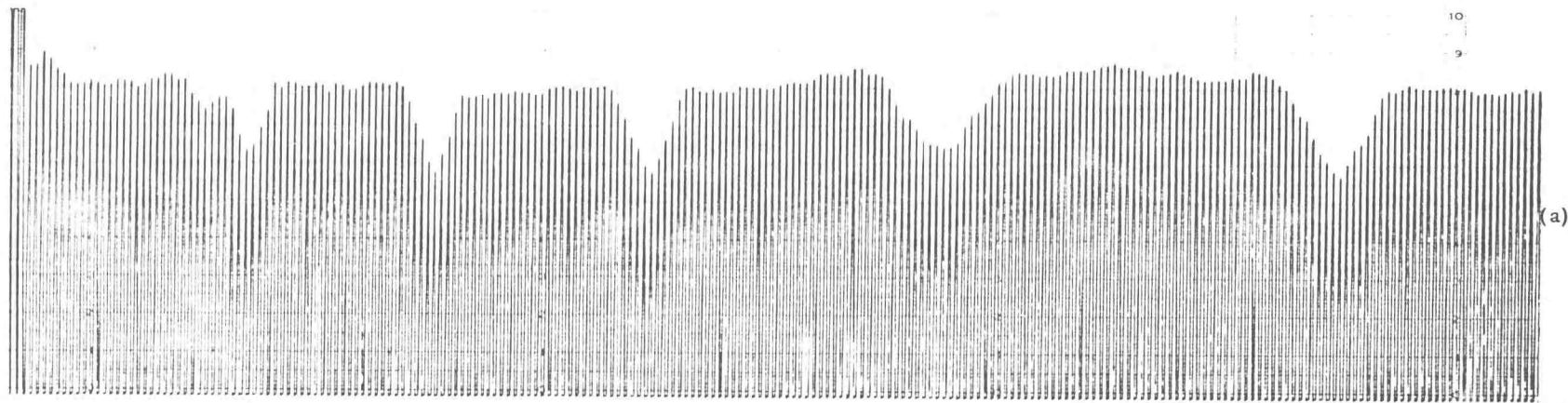


Figure 57. Autocorrelation of Figure 56(a) and (b). Vertical - 50m volts/division. Horizontal - 18sec/division.

If the line fault is an open circuit any pulse sent down the line will be reflected (1,p.209) and appear at the input T seconds later.

The value of T is proportional to the propagation velocity of the transmission line and the distance the fault is from the input. An example of one possible waveform that would result from pulsing an open circuit line is shown in Figure 58.

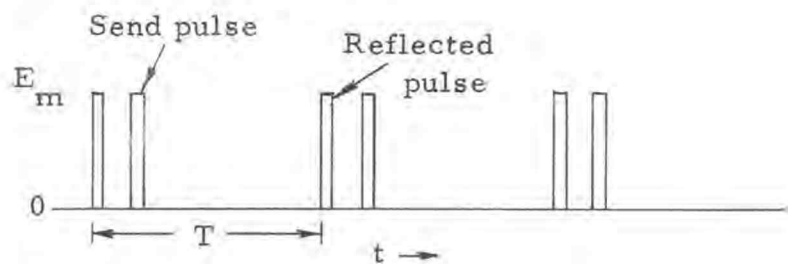


Figure 58. Voltage waveform for pulsed communications line terminated with open circuit.

Correlation would not be necessary unless the periodic pulse train were masked with noise. Excessive noise on a faulted line is a common problem. By autocorrelating the waveform in Figure 58 masked with noise the value of T can be determined from $\phi_{11}(T)$. Once T is calculated the distance to the line fault can be computed knowing the characteristics of the line.

Two important limitations regarding autocorrelation of a periodic pulse train (no noise) with this correlator are:

1. The rms voltage of the pulse train should be kept above 0.4 volts.

2. The pulse width of each pulse should
be at least $25\mu\text{sec}$

It should also be mentioned that autocorrelation of a periodic pulse train does not produce perfect triangles, as evidenced in Figure 57. The sharp corners and peaks of each triangle are lost due to the upper frequency limit of the correlation.

The frequency spectrum for a pulse train is shown in Figure 59.

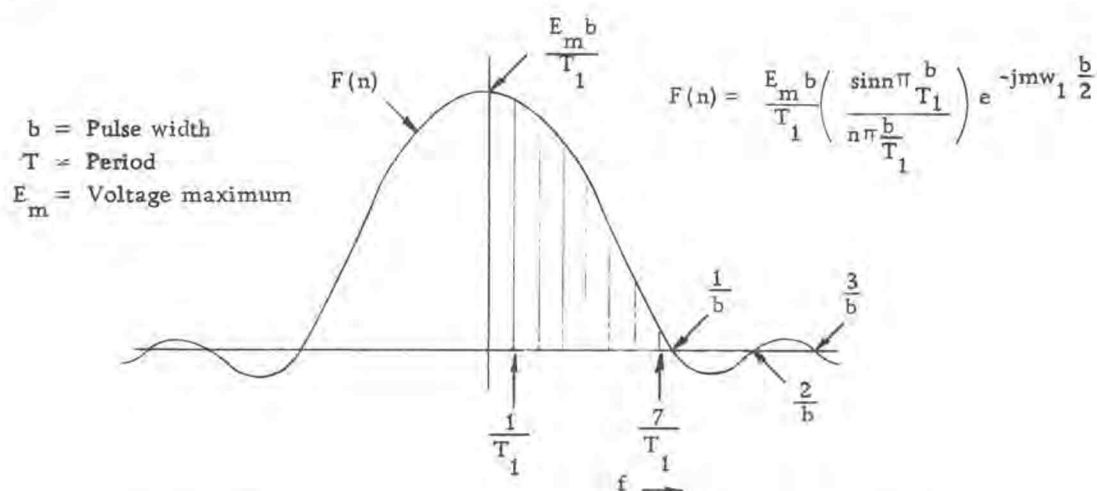


Figure 59. Frequency spectrum of periodic waveform of rectangular pulses.

The pulse train in Figure 56 has a pulse width of $25\mu\text{sec}$ and pulse repetition rate of 5700 pps. Only the fundamental frequency $(1/T_1)$ and 2nd - 7th harmonics will appear in the correlator output due to its upper frequency limit of 40kc. The triangle peaks and sharp corners are produced by frequencies above 40kc, which are lost.

IN RETROSPECT

If the circuit were to be designed again with the added knowledge gained from building the original system there are several changes that would be made.

The first is a suggestion that would apply to any system of complex circuitry. The value of B^+ and B^- should be increased to at least +20 v instead of the +12 v bias used. This allows greater flexibility for sweep generators, d. c. amplifiers, and most important would allow a greater pk - pk value of input signal without saturating the sampler.

A linear voltage step generator is needed. The system works fine with the exponential step generator now being used, but it is more difficult to accurately calculate the frequency, or pulse width, of $\phi_{11}(\tau)$. If the value of τ_k were constant over all values of τ , the frequency of $\phi_{11}(\tau)$ could be read directly from the recorded data.

CONCLUSION

The application of correlation to detect periodic signals in random noise, using solid state circuitry, has been successfully completed.

The correlator will operate from 2kc-30kc with excellent results. Periodic sinusoids and pulse trains were detected with the N/S ratio as high as 10db ($N_{rms} = 3.14S_{rms}$). This corresponds to 16db when the signal and noise are measured in peak values. The system is reliable in operation, inexpensive to build, simple to operate, and due to solid state components is durable and compact. The most expensive components used in the circuit are the field effect transistors. Without them, however, the system would have been much more difficult to build. A solid state device with very high input impedance was required and the FET filled this requirement. No high speed switching transistors or diodes are required which helps keep the cost at a minimum.

The system is by no means perfected. With the following circuit refinements the frequency response could be increased to 2kc-75kc and signals could probably be detected with the N/S ratio as high as 20db.

1. Take more sample pairs (increase N).
2. Reduce T_k .

3. Reduce the time needed to sample $f_1(t)$.

The concept of detecting periodic signals in random noise by autocorrelation has been shown to be both practical and feasible in this study. The correlators application to line fault location is only one of many possible applications of this system.

BIBLIOGRAPHY

1. Albert, A. L. Electrical communication. New York, John Wiley and Sons, 1959. 593 p.
2. Fitchen, Franklin C. Transistor circuit analysis and design. New York, D. Van Nostrand, 1960. 356 p.
3. Kuo, Tsung-i. Analysis and synthesis of sampled-data control systems. Englewood Cliffs, N.J., Prentice Hall, 1963. 528 p.
4. Lee, Y. W. Statistical theory of communications. New York, John Wiley and Sons, 1960. 509 p.
5. Malmstadt, H. V. Electronics for scientists. New York, W. A. Benjamin, 1962. 619 p.
6. Reintjes, F. J. An analogue electronic correlator. Proceedings of the National Electronics Conference 7: 390-400. 1951.
7. Senk, F. M. Jr. The design and evaluation of an electronic estimation of probability density distributions. Master's thesis. Corvallis, Oregon State University, 1964. 102 numb leaves
8. Strauss, Leonard. Wave generation and shaping. New York, McGraw-Hill, 1960. 520 p.
9. Texas Instruments Inc. Transistor circuit design. New York, McGraw-Hill, 1963. 523 p.

APPENDICES

APPENDIX I

Important Basic Circuits and Calculations

The following discussion covers any circuit or calculation referred to in the body of the thesis.

Maximum Allowable Leakable Current (L_c) for Sampler-A

If the sampler accuracy is to be within five per cent, the leakage current must remain small for the period of time T_7 is OFF. (1.3 msec).

If the maximum voltage C_s charges to is +7 volts, five per cent accuracy allows a change in capacitor voltage of 0.35 volts. From this information the maximum allowable leakage current is calculated.

$$\begin{aligned}
 C &= \frac{Q}{V} \\
 Q_{\max} &= CV = (50 \text{ pfd}) (0.35\text{v}) \\
 &= 17.0 \times 10^{-12} \text{ coulombs} \\
 L_c &\leq \frac{Q_{\max}}{T} \leq \frac{17.0 \times 10^{-12} \text{ coulombs}}{1.3 \text{ msec}} \\
 &\leq 13.0 \times 10^{-9} \\
 &\leq \underline{\underline{13 \text{ nanoamps}}}
 \end{aligned}$$

Field Effect Transistors

FET (5, p.149) are a high input impedance solid state voltage amplifier. The output characteristics are similar to a vacuum tube pentode.

A P-channel FET with normal bias, and its equivalent circuit, are shown in Figure 60.

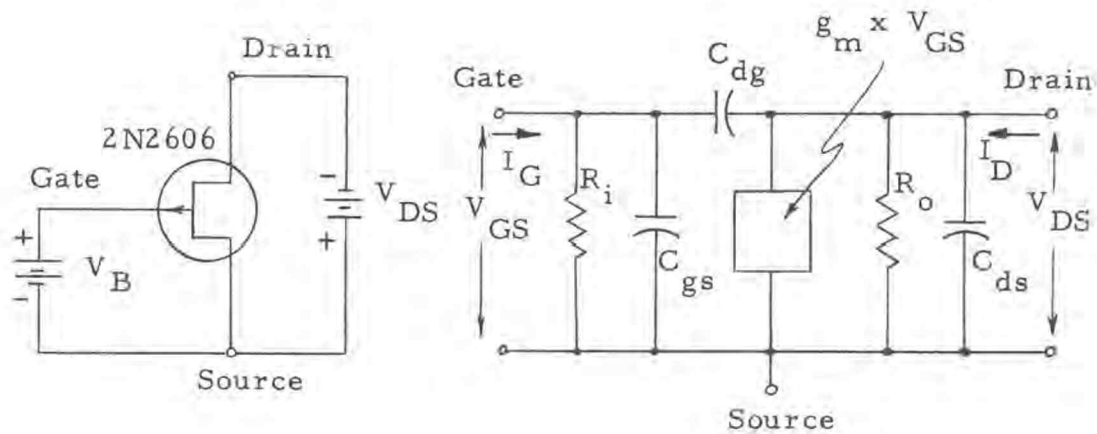


Figure 60. FET and its equivalent circuit.

The transconductance, g_{ms} is defined as

$$g_m = \left. \frac{\partial I_d}{\partial V_g} \right|_{V_d = K}$$

V_g = Gate to ground voltage

V_d = Drain to ground voltage

The input impedance, R_i , is equal to that of a reverse biased diode. For Siliconix 2N2606 this value is equal to 2000 meg Ω .

The value of R_o is obtained by determining the slope of the output characteristic curves at the operating point (small signal operation).

Miller Sweep Generator Reset Circuit

Miller sweep generator -1 is shown in Figure 61. The switch S resets the capacitor to B^+ whenever closed. When open it allows C to discharge.

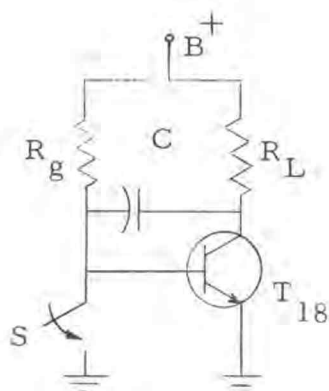


Figure 61. Miller sweep generator-1.

The electronic switching transistor shown in Figure 62 is used for S . This switch is activated each time the monostable pulse generator (PG) is triggered. The width of the pulse produced by PG is adjusted to turn S on long enough to charge C completely. When T_{17} comes ON the base of the sweep generator transistor becomes equal to B^+ , which turns T_{18} OFF and C discharges

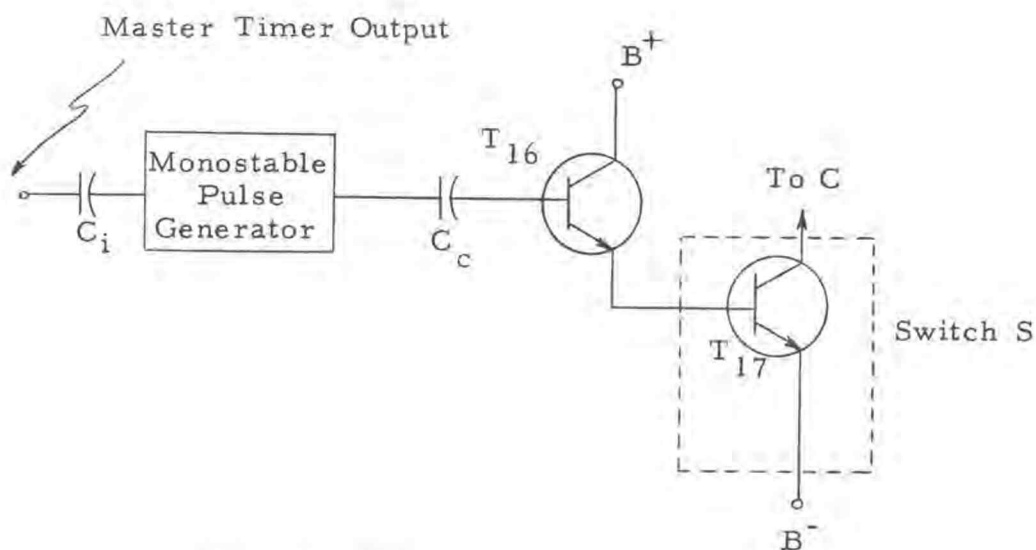


Figure 62. Miller sweep generator-1 reset.

toward B^- . This allows the collector voltage on T_{18} to return to B^+ . The darlington configuration of T_{16} and T_{17} is to insure T_{17} is being turned ON enough to saturate. T_{17} turns OFF immediately when the switching pulse is removed.

APPENDIX II

Correlator Test Operation Instructions

The correlator operation is entirely automatic once a few minor adjustments are made. The following procedure is presented to help the operator in making these adjustments so proper correlation takes place. It is assumed that all portions of the system are operating correctly. Refer to the circuit diagram in Appendix V for terminal connections.

Required Test Equipment

1. Good quality cathode ray oscilloscope (CRO), such as Tektronix 531 or 545.
2. Strip chart recorder with the following specifications.
 - a. Chart speed of ≈ 1 inch/70 sec.
 - b. Minimum frequency response or 100 cps.
 - c. Sensitivity of 1 volt/chart width or more.
 - d. Zero suppression.
3. Signal generator that will supply frequencies from 2kc - 40kc.

Test Operation

1. Adjust all bias voltages to values listed in circuit specifications, Appendix III. Allow 5 minutes for circuit and test equipment to warm up.
2. Adjust CON-1 until the d.c. voltage at the integrator input is exactly zero.
3. Close switch S.
4. Connect 10kc sinusoidal signal to $f_1(t)$ and $f_2(t)$ input terminals.
5. Connect strip chart recorder to correlator output and adjust chart speed to approximately 1 inch/70 sec.
6. Open switch S and autocorrelation of 10kc signal will proceed automatically.
7. The value of $\phi_{11}(\tau)$ will be monitored by the strip chart recorder. The d.c. level at the output is approximately -6 volts and the a.c. variation $(\phi_{11}(\tau))$ 0.3 to 0.4. Use zero suppression and clamping (E_o and D_o) to remove d.c. level and leave just $\phi_{11}(\tau)$.
8. Correlation can run as long as desired; up to 20 min maximum. To stop correlation close switch S which resets τ to zero shift.

This completes the test operation procedure. The output should be a smooth sinusoidal signal as shown in Figure 36-40, pages 59, 60, 61.

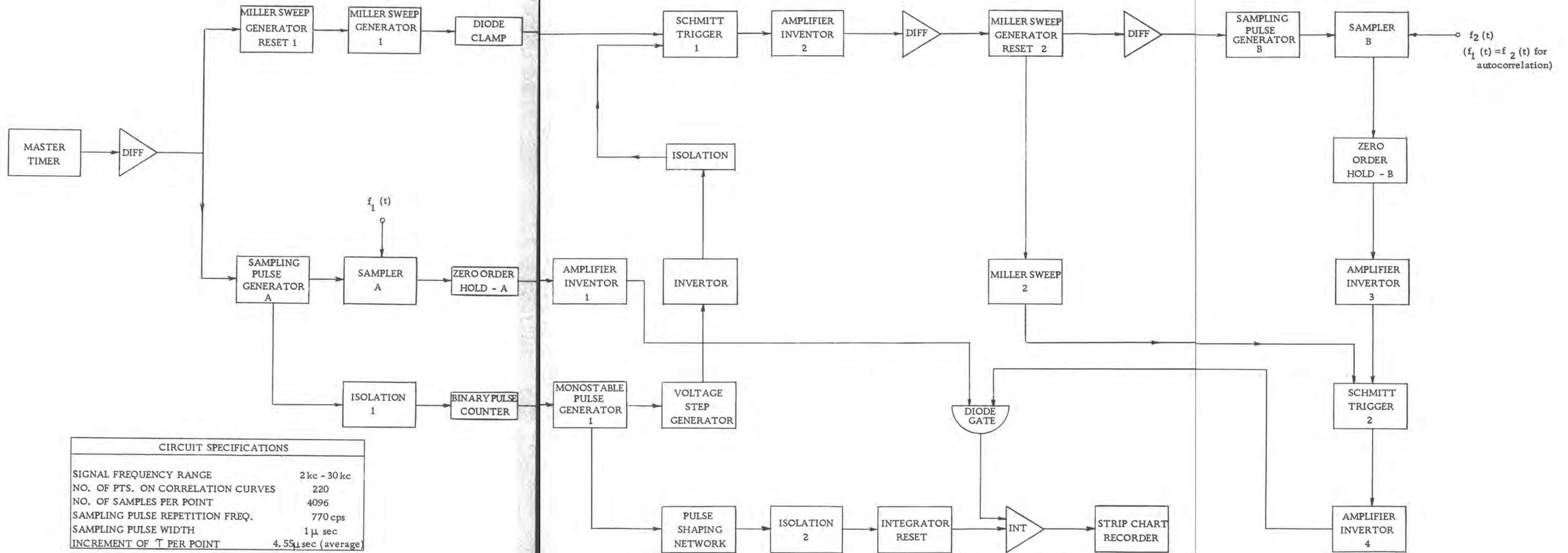
APPENDIX III

Circuit Specifications

| | |
|--|--|
| 1. Frequency response | 2kc - 30kc |
| 2. Total time delay, τ | 1 msec |
| 3. Delay steps, τ_k | 4.55 μ sec |
| 4. Total number of points on correlation curve | 220 |
| 5. Total correlation time | 20 minutes |
| 6. Maximum input N/S ratio | 10 db |
| 7. Input voltage level | 0.4 v _{rms} minimum signal level |
| 8. Power requirements | 120 vac, 60 cps + 12 v.d.c. 100 ma - 12 v.d.c. 250 ma + 25 v.d.c. 10 ma |

APPENDIX IV

Figure 63. Complete Block Diagram
of Medium Frequency Solid
State Correlator.



APPENDIX V

Figure 64. Complete Circuit Diagram
of Medium Frequency Solid
State Correlator.

